Tiempo de vida de portadores minoritarios

$$\tau_r = (Bn)^{-1}$$

GaAs a 300 K

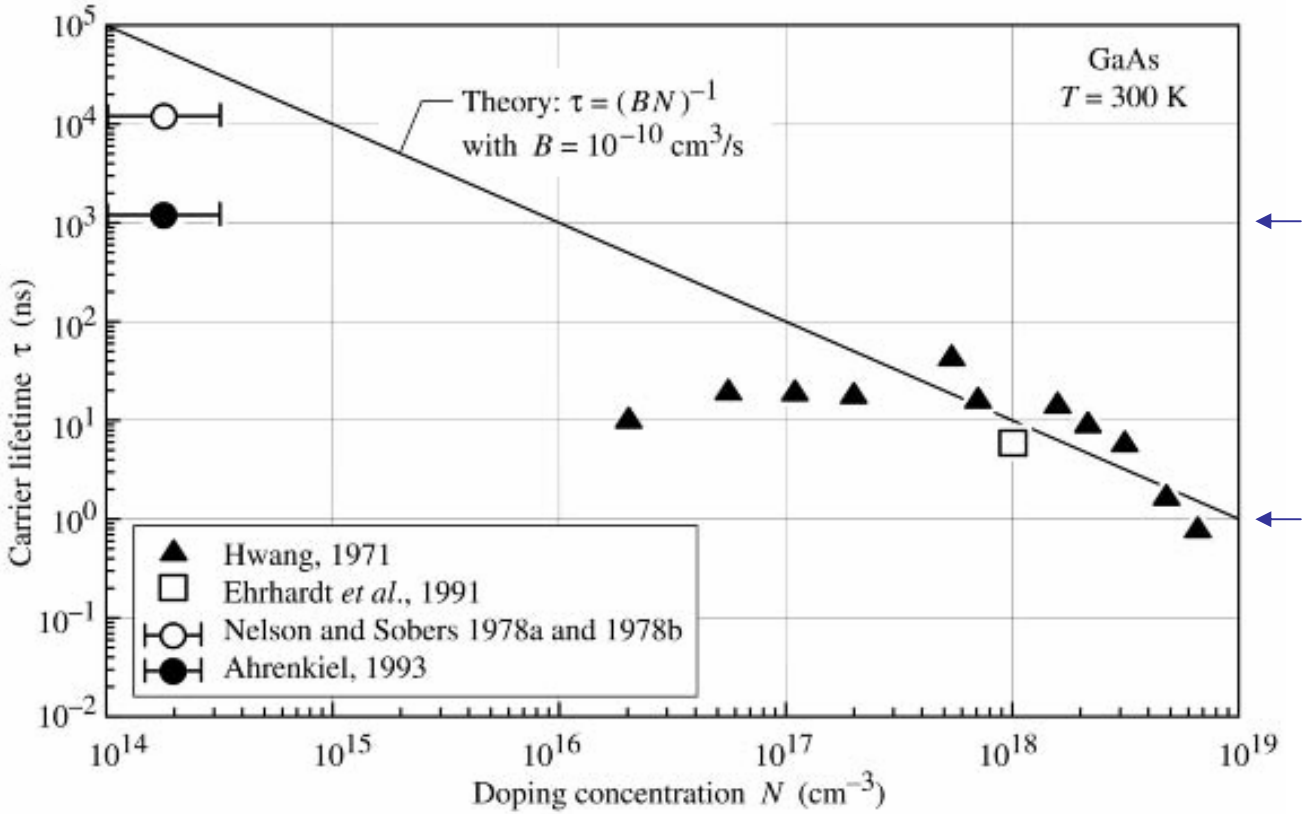

← 1 µs

← 1 ns

Fig. 1.3. Minority carrier lifetime as a function of doping concentration in GaAs at 300 K. The lifetime was inferred from luminescence decay mesurements. The data points of Nelson and Sobers (1978a and 1978b) and Ahrenkiel (1993) were measured on nominally undoped material with a doping concentration $<< 10^{15}$ cm^{-3}.

Tiempo de vida disminuye con dopaje

Ritmo en GaAs y Si

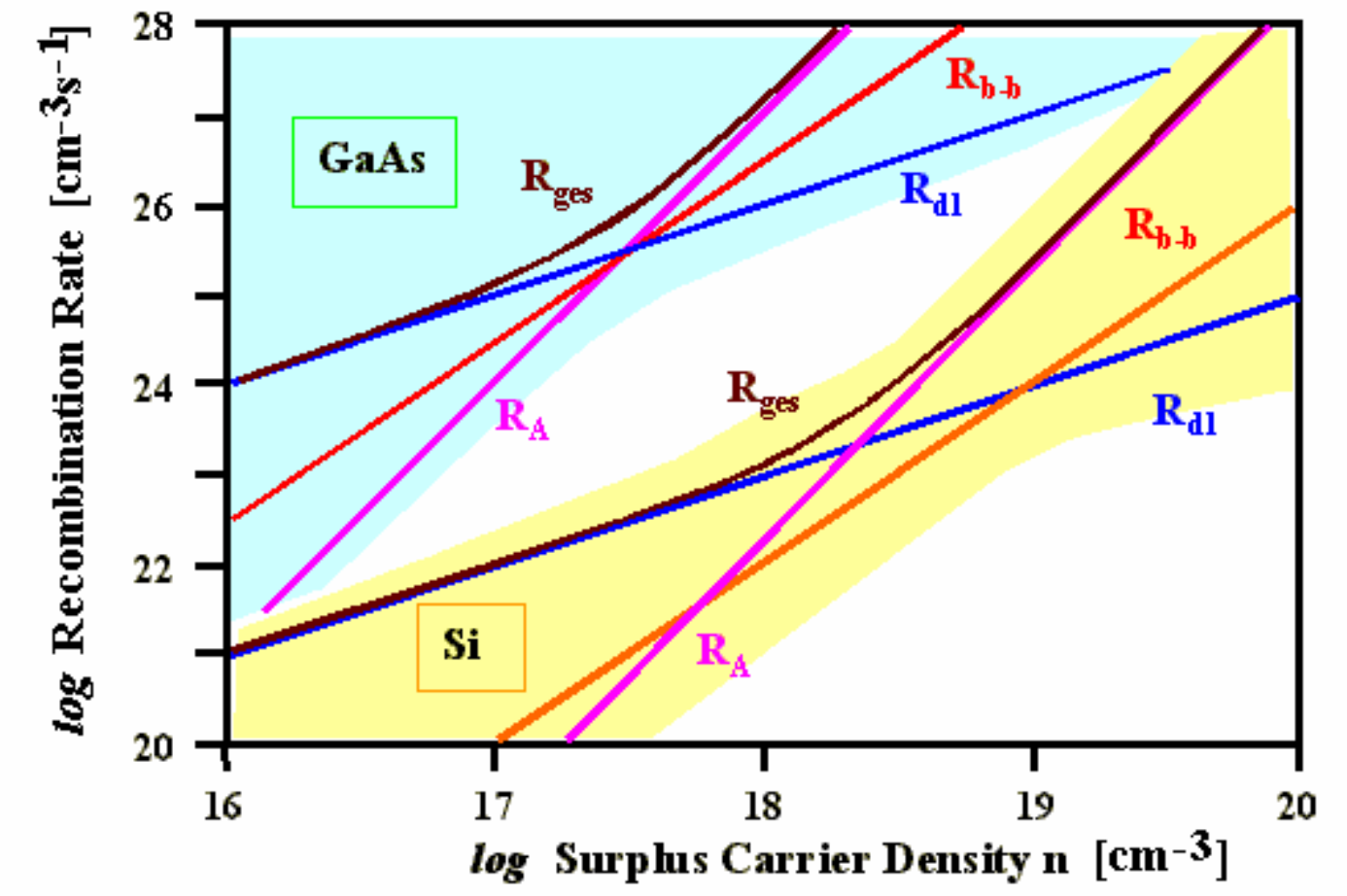

radiativa

$R_{b\text{-}b}$ interbanda

no-radiativa

R_{dl} nivel profundo

R_A Auger

Eficiencia

Eficiencias de

- inyección η_{in} la parte de la corriente creando portadores minoritarios para recombinar →
- recombinación (interna) η_r $\eta_r = R_r / \left(R_r + R_{nr}\right)$
- extracción η_e nº fotones emitido al exterior / total emitido

Total (conversión externa)

$$\eta_0 = \eta_{in}\,\eta_r\,\eta_e$$

$$\eta_0 = \eta_{externa} = \frac{P_{out}(\text{Optical})}{IV}$$

Eficiencia de materiales LED

Selected LED semiconductor materials. Optical communication channels are at 850 nm (local network) and at 1.3 and 1.55 μm (long distance). D = direct, I = Indirect bandgap. DH = Double heterostructure. $\eta_{external}$ is typical and may vary substantially depending on the device structure.

Semiconductor	Substrate	D or I	λ (nm)	$\eta_{external}$ (%)	Comment
GaAs	GaAs	D	870 - 900	10	Infrared LEDs
$Al_xGa_{1-x}As$ ($0< x < 0.4$)	GaAs	D	640 - 870	5 - 20	Red to IR LEDs. DH
$In_{1-x}Ga_xAs_yP_{1-y}$ ($y \approx 2.20x$, $0 < x < 0.47$)	InP	D	1 - 1.6 μm	> 10	LEDs in communications
InGaN alloys	GaN or SiC Saphire	D	430 - 460	2	Blue LED
			500 - 530	3	Green LED
SiC	Si; SiC	I	460 - 470	0.02	Blue LED. Low efficiency
$In_{0.49}Al_x\ Ga_{0.51-x}\ P$	GaAs	D	590 - 630	1 - 10	Amber, green red LEDs
$GaAs_{1-y}P_y$ ($y < 0.45$)	GaAs	D	630 - 870	< 1	Red - IR
$GaAs_{1-y}P_y$ ($y > 0.45$) (N or Zn, O doping)	GaP	I	560 - 700	< 1	Red, orange, yellow LEDs
GaP (Zn-O)	GaP	I	700	2 - 3	Red LED
GaP (N)	GaP	I	565	< 1	Green LED

Eficiencia de inyección η_{in}

Corriente a través de la unión p-n en polarización directa

$$j = j_h(0^+) + j_e(0^-) = q\left(\frac{D_h p_{N0}}{L_h} + \frac{D_e n_{P0}}{L_e}\right)\left(e^{\frac{qV}{kT}} - 1\right)$$

Para sólo inyección de <u>electrones</u> en capa p

$$\frac{\text{Electrones inyectados en la parte p}}{\text{Corriente total}} = \eta_{in} = \frac{j_e(0^-)}{j_h(0^+) + j_e(0^-)} = \frac{\frac{D_e n_{P0}}{L_e}}{\frac{D_h p_{N0}}{L_h} + \frac{D_e n_{P0}}{L_e}}$$

Eficiencia de inyección η_{in}

Para sólo inyección de <u>electrones</u> en capa p

$$\eta_{in} = \frac{1}{1+\frac{D_h L_e\, p_{N0}}{D_e L_h n_{P0}}} \approx \frac{1}{1+\frac{\mu_h\, p_{P0}}{\mu_e n_{N0}}}$$

con $\mu_e >> \mu_h$

$L_e \approx L_h$

$n_P p_P = n_N p_N = n_i^2$

$\Rightarrow \eta_{in} \cong 1$ mas alta con $n_N >> p_P$ capa n mas dopado

Dispositivo con sólo inyección de electrones η_{in}

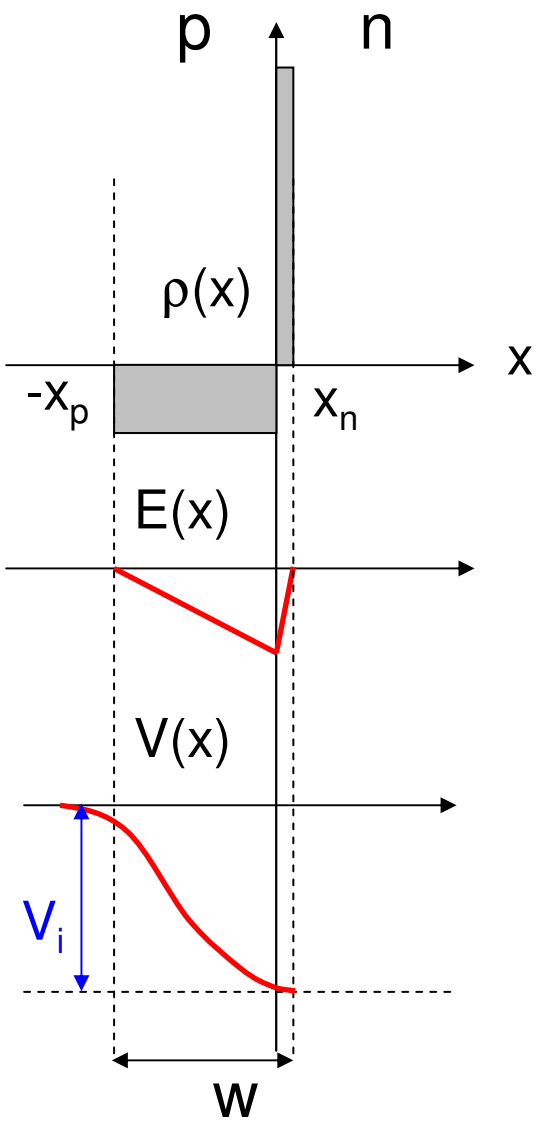

LED Asimétrico:

Unión n^+-p : N_D (capa n) >> N_A (capa p)

$$N_D x_n = N_A x_p \quad \Rightarrow \quad V_p >> V_n$$

Realización de $n_N >> p_P$

Sólo importan para la recombinación electrones minoritarios inyectados en capa p

Union n+-p : Surface-emitting LED

η_{in}

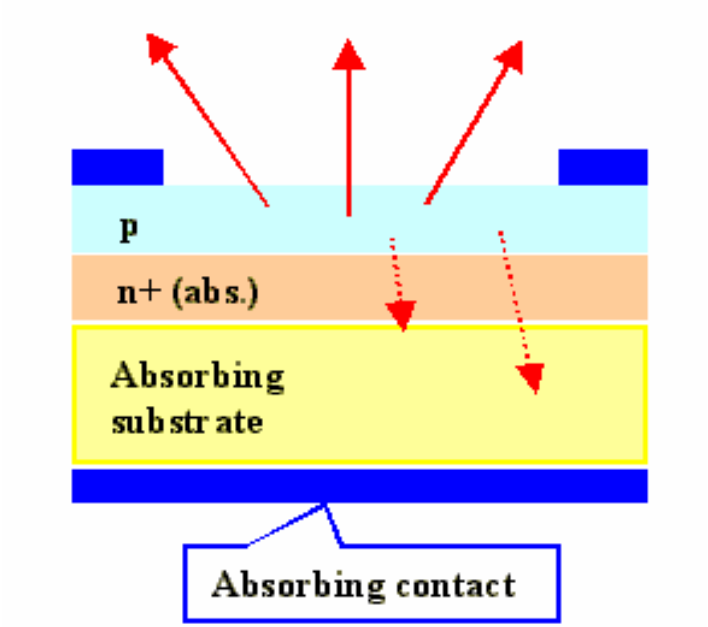

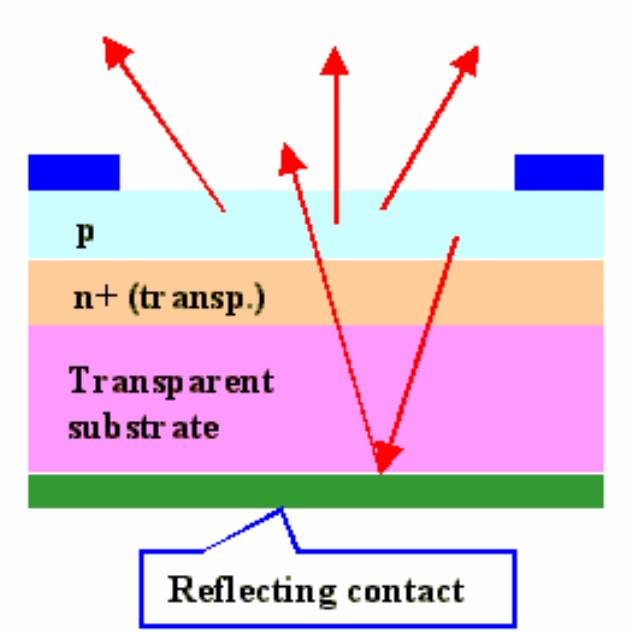

simple y barato

por ejemplo:
- con emisión de excitones (GaP)
- heterouniones

energía emisión < energía gap

Eficiencia de Recombinación η_r

$$\eta_r = R_r / \left(R_r + R_{nr} \right)$$

Materiales de gap directo (homounión) ~ 50%

- electrones entran profundo en región activa
- fotones reabsorbidos
- fotones emitidos hacia dentro del LED

Materiales de gap indirecto: pequeño

con impurezas profundas: GaP:Zn, O: ~ 30%
GaP:N ~ 3%

Estructuras de Doble Heterounión: 60 - 80%

Eficiencia de extracción

η_e

Limitado por:

1. Reabsorción

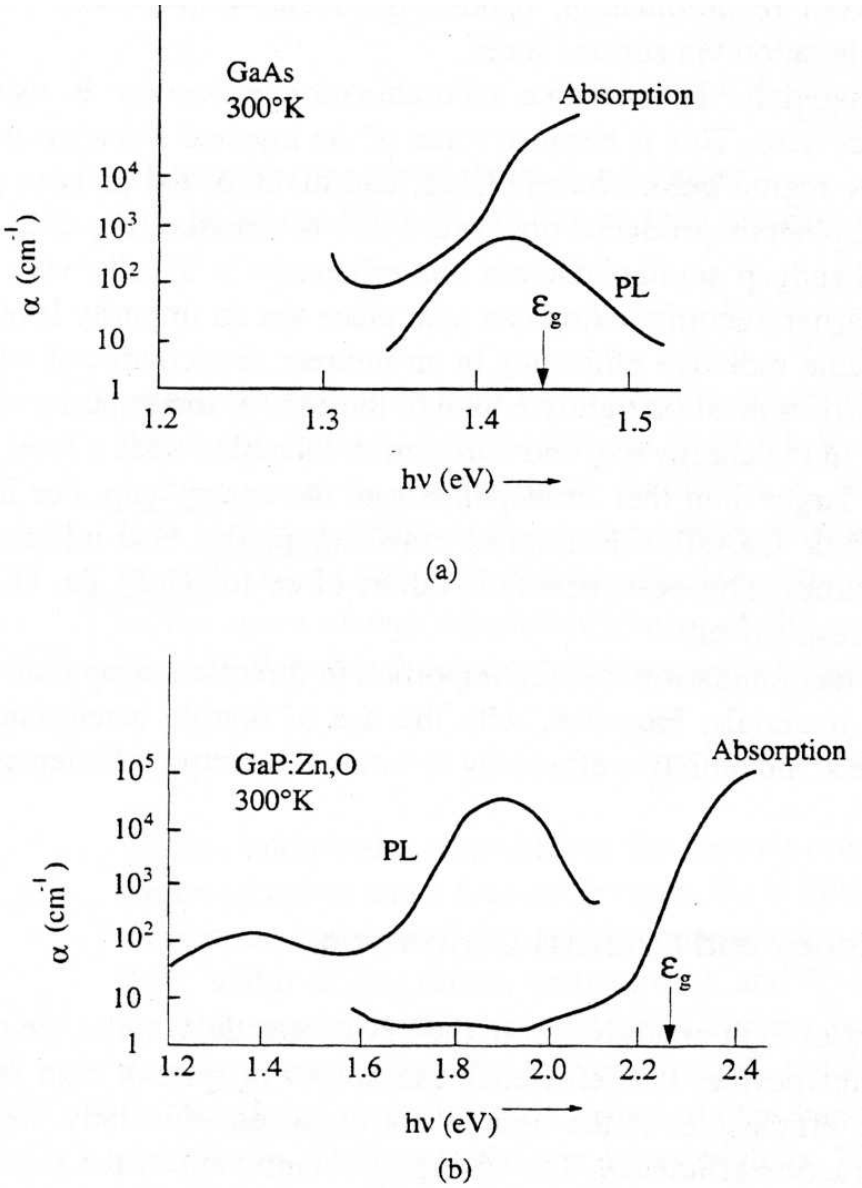

Eficiencia de extracción η_e

Limitado por:

2. Geometría de radiación del LED
   (fotones emitidos con $\theta > \theta_c$ atrapados)

$$\theta_c = \sin^{-1}(n_2 / n_1)$$

Para GaAs n=3.6 θ_c=17º

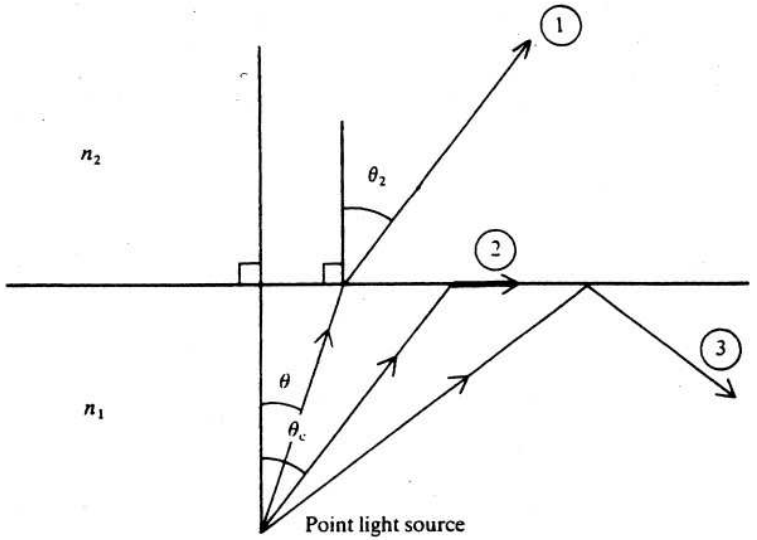

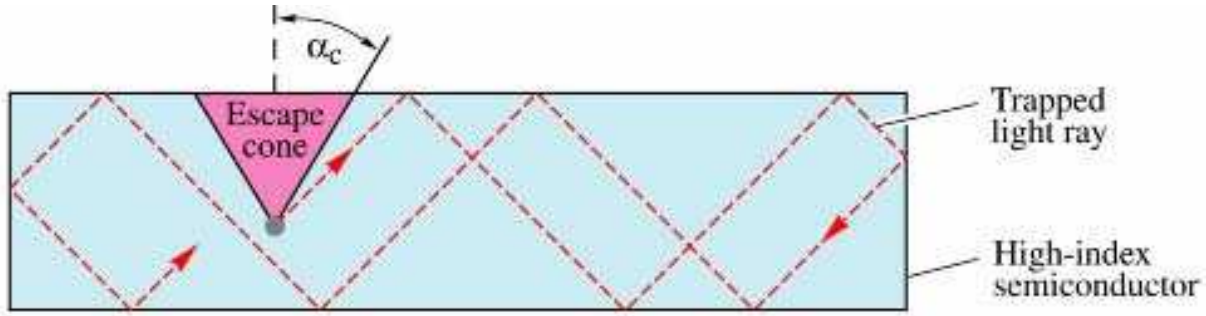

Fig. 6.3. Illustration of "trapped light" that cannot escape from a cube-shaped semiconductor for emission angles larger than α_c due to total internal reflection.

Eficiencia de extracción η_e

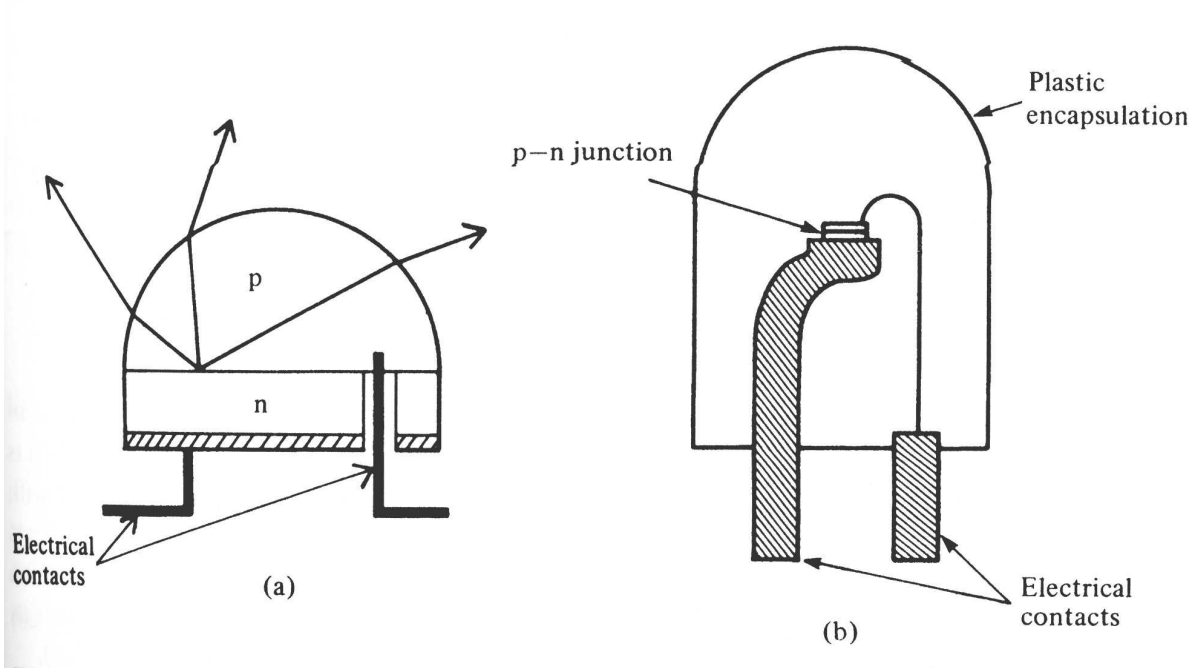

Fracción transmitida a medio 2

$$F = \frac{1}{4}\left(\frac{n_2}{n_1}\right)^2\left[1-\left(\frac{n_1-n_2}{n_1+n_2}\right)^2\right]$$

GaAs: n_1=3.6, n_2=1 (aire) $F \approx 0.013$

n_2=1.5 (plástico) $F \approx 0.036$

Distribución angular de Intensidad η_e

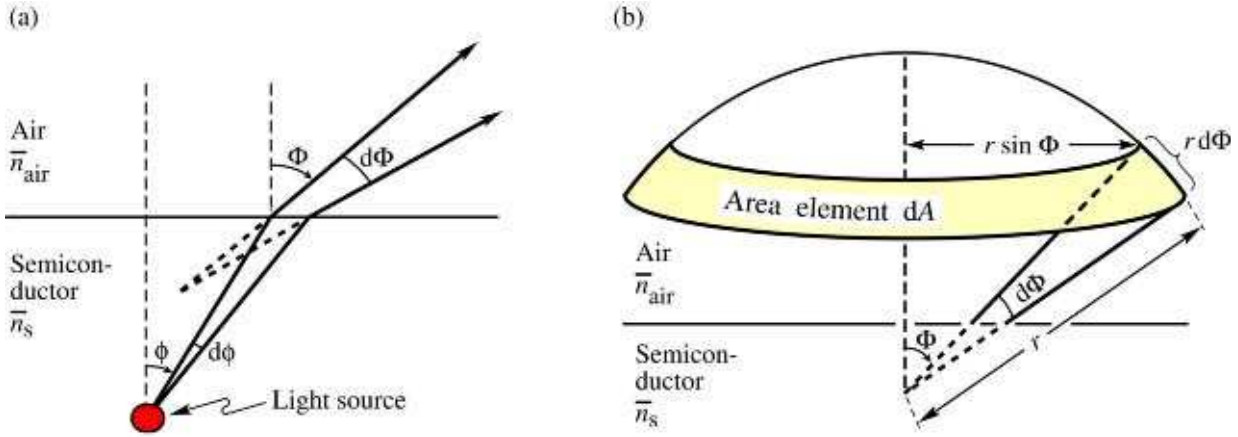

Fig. 4.4. Geometrical model used to derive the Lambertian emission pattern. (a) The light emitted into angle dϕ inside the semiconductor is emitted into the angle dΦ in air. (b) Illustration of area element dA of the calotte.

Distribución angular de Intensidad η_e

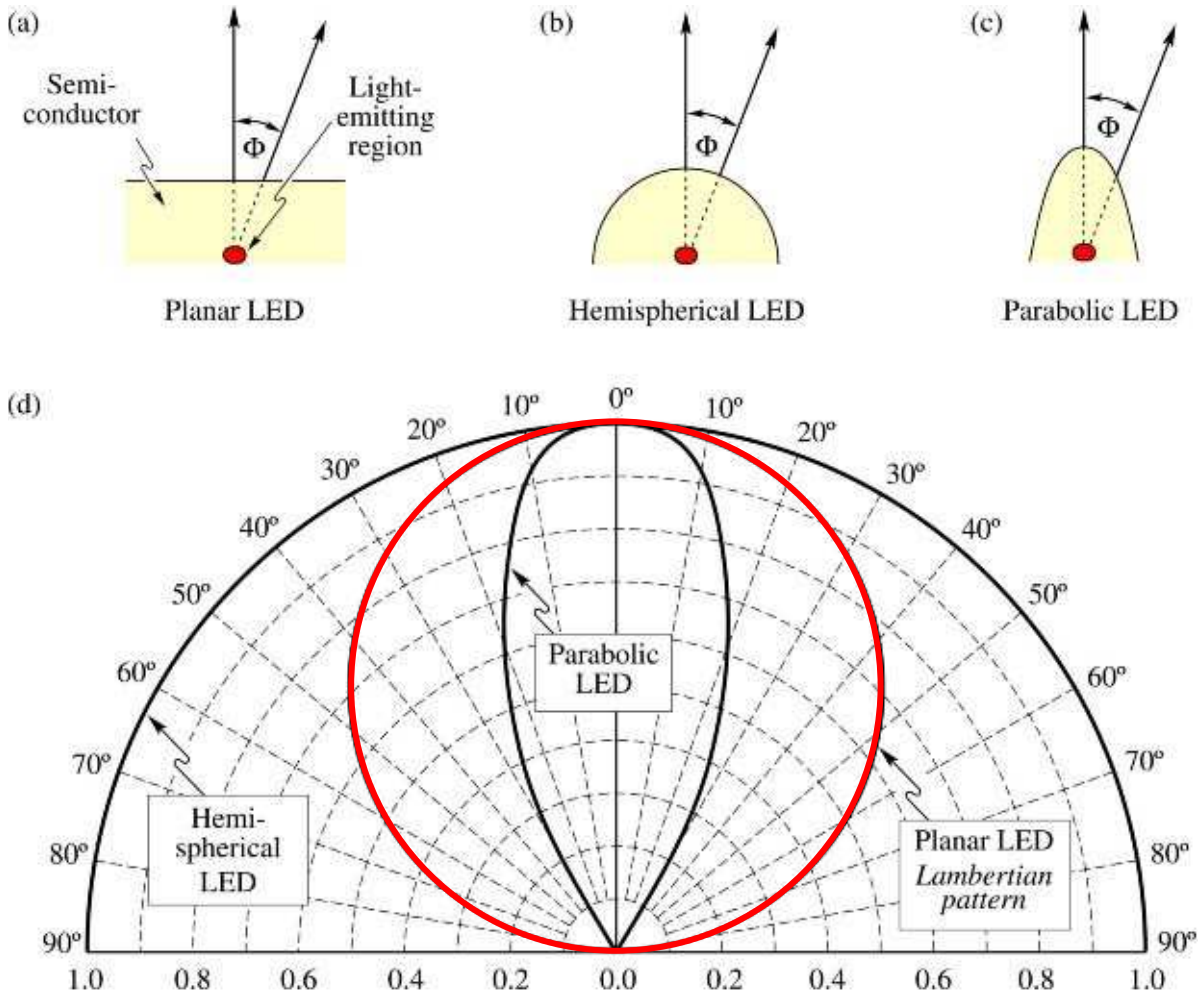

Fig. 4.5. Light-emitting diodes with (a) planar, (b) hemispherical, and (c) parabolic surfaces. (d) Far-field patterns of the different types of LEDs. At an angle of $\Phi = 60°$, the Lambertian emission pattern decreases to 50 % of its maximum value occuring at $\Phi = 0°$. The three emission patterns are normalized to unity intensity at $\Phi = 0°$.

LED planar:

Lambertian

$I = I_0 \cos \Phi$

Eficiencia de extracción

η_e

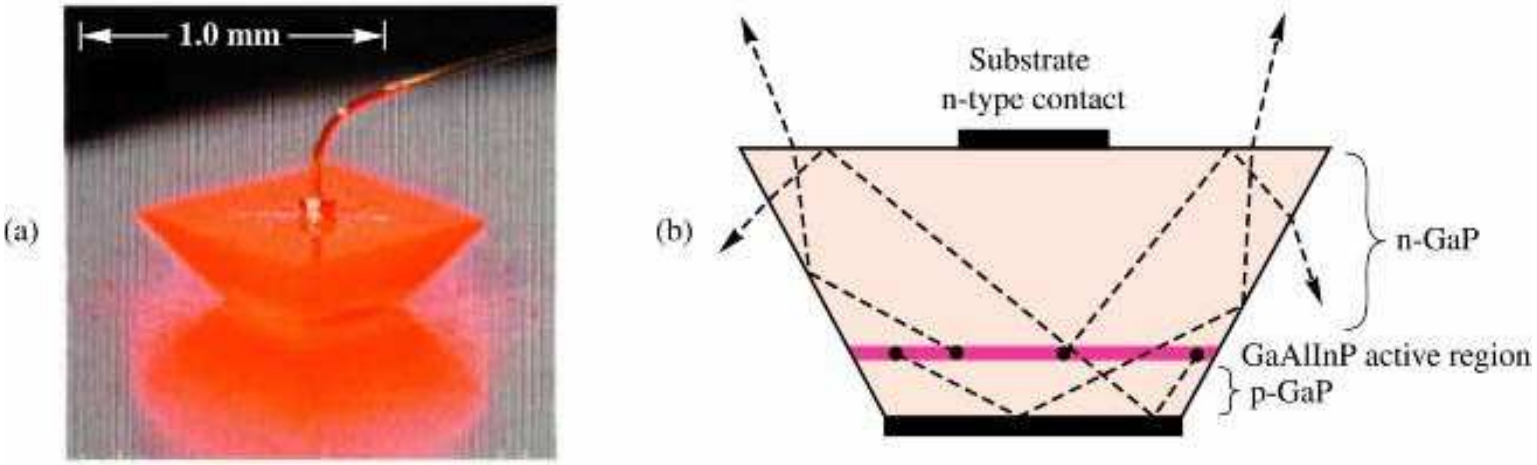

Fig. 6.6. Truncated inverted pyramid (TIP) AlInGaP/GaP LED. (a) LED driven by an electrical injection current. (b) Schematic diagram of the LED illustrating the enhanced light extraction efficiency (after Krames *et al.*, 1999).

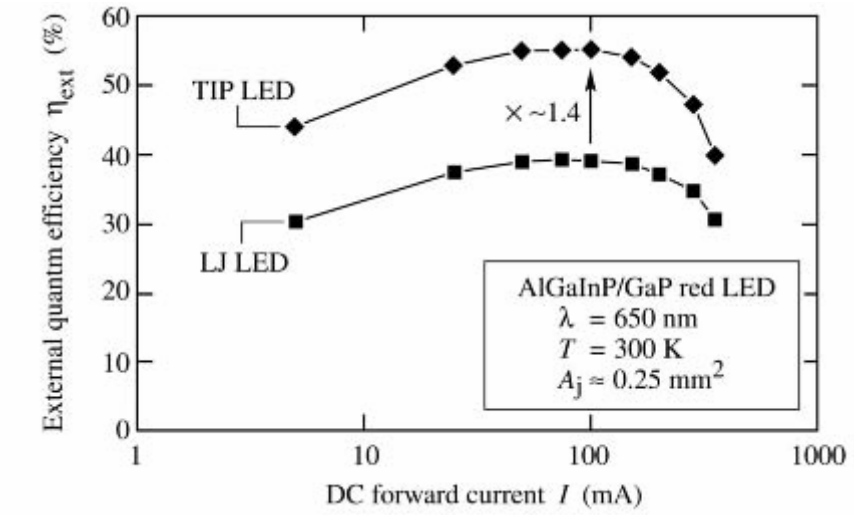

Eficiencia externa TIP-LED vs. LED convencional (Large Junction)

Recombinación en gap indirecto- GaAsP

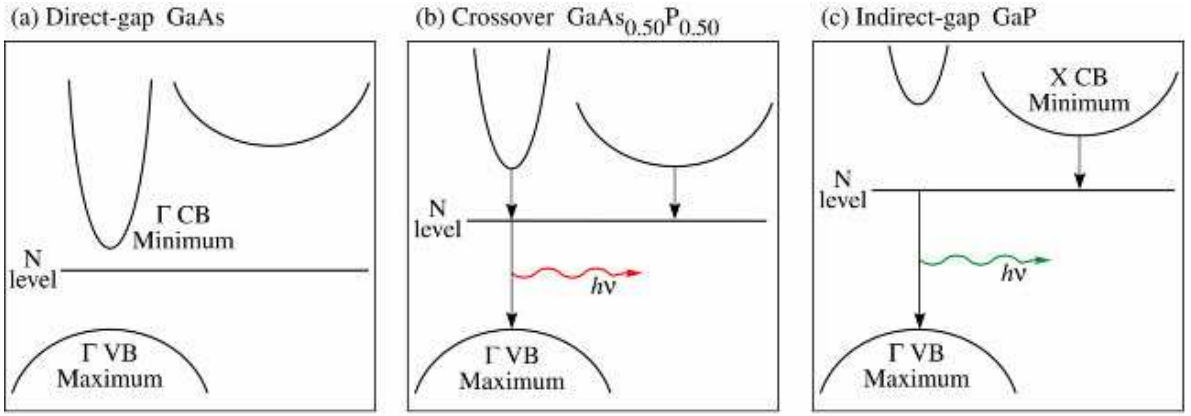

nivel N

Fig. 7.1. Schematic band structure of GaAs, GaAsP, and GaP. Also shown is the nitrogen level. At a P mole fraction of about 45 - 50 %, the direct-indirect crossover occurs.

Energía de emisión

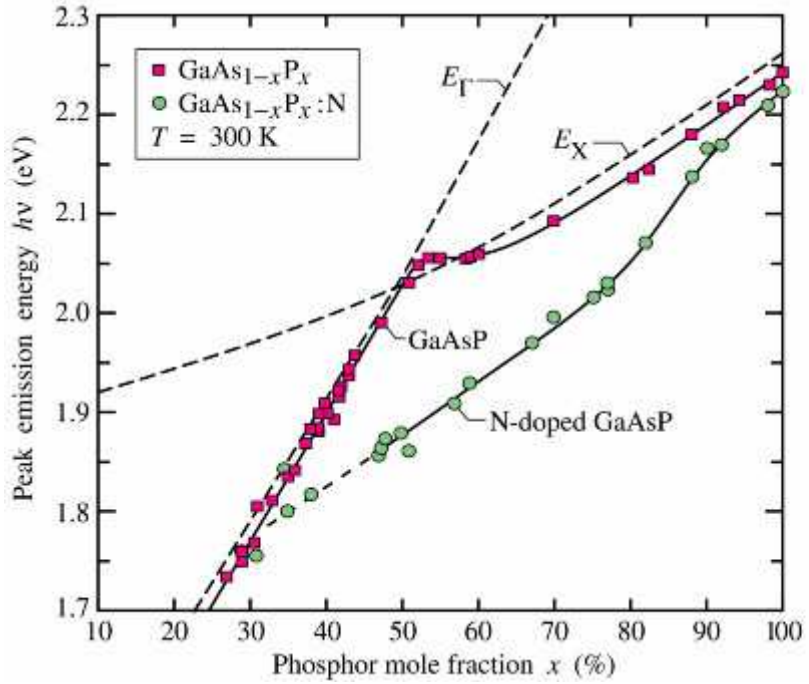

Fig. 7.2. Room - temperature peak emission energy versus alloy composition for undoped and nitrogen - doped GaAsP light - emitting diodes injected with a current density of 5 A / cm^2. Also shown is the energy gap of the direct (E_Γ) and indirect (E_X) transition. The direct-indirect crossover occurs at $x \approx 50$ % (after Craford *et al.* 1972).

Eficiencia externa (total)

η_0

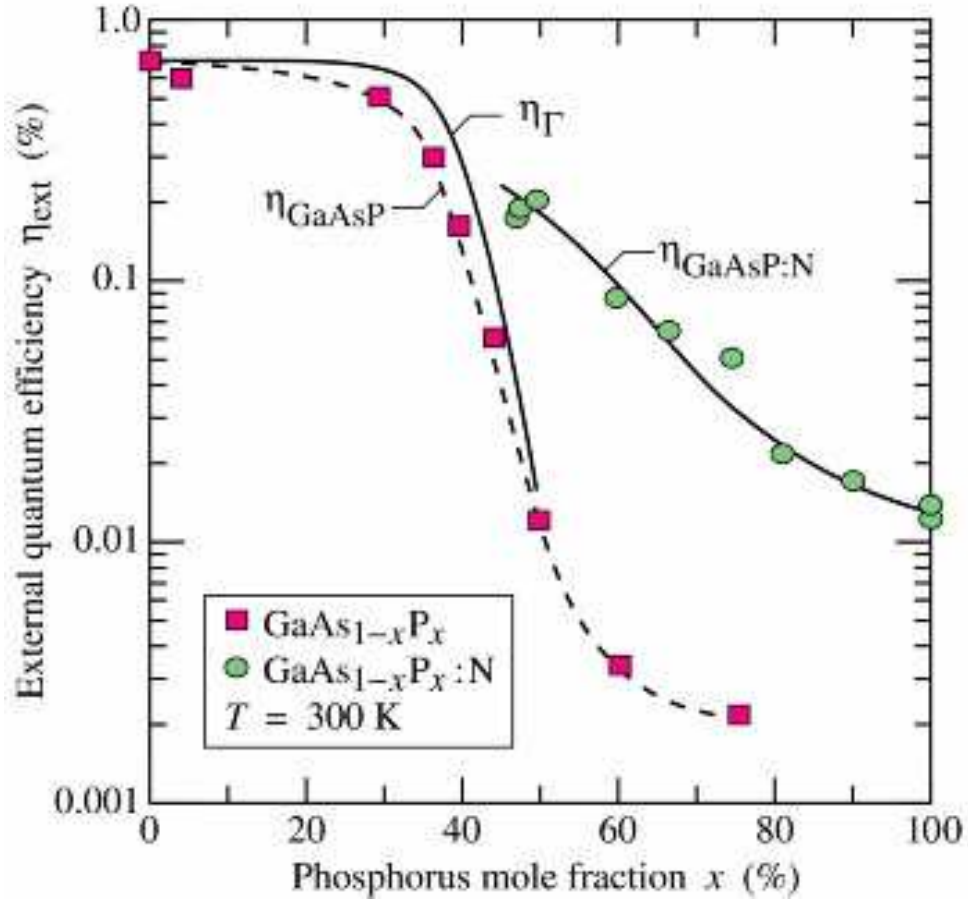

Fig. 7.3. Experimental external quantum efficiency of undoped and N-doped GaAsP versus P mole fraction. Also shown is the calculated direct-gap (Γ) transition efficiency, η_Γ, and the calculated nitrogen (N) related transition efficiency, η_N (solid lines). Note that the nitrogen-related efficiency is higher than the direct-gap efficiency in the indirect bandgap (x > 50 %) regime (after Campbell *et al.*, 1974).

Eficiencia externa (total)

η_0

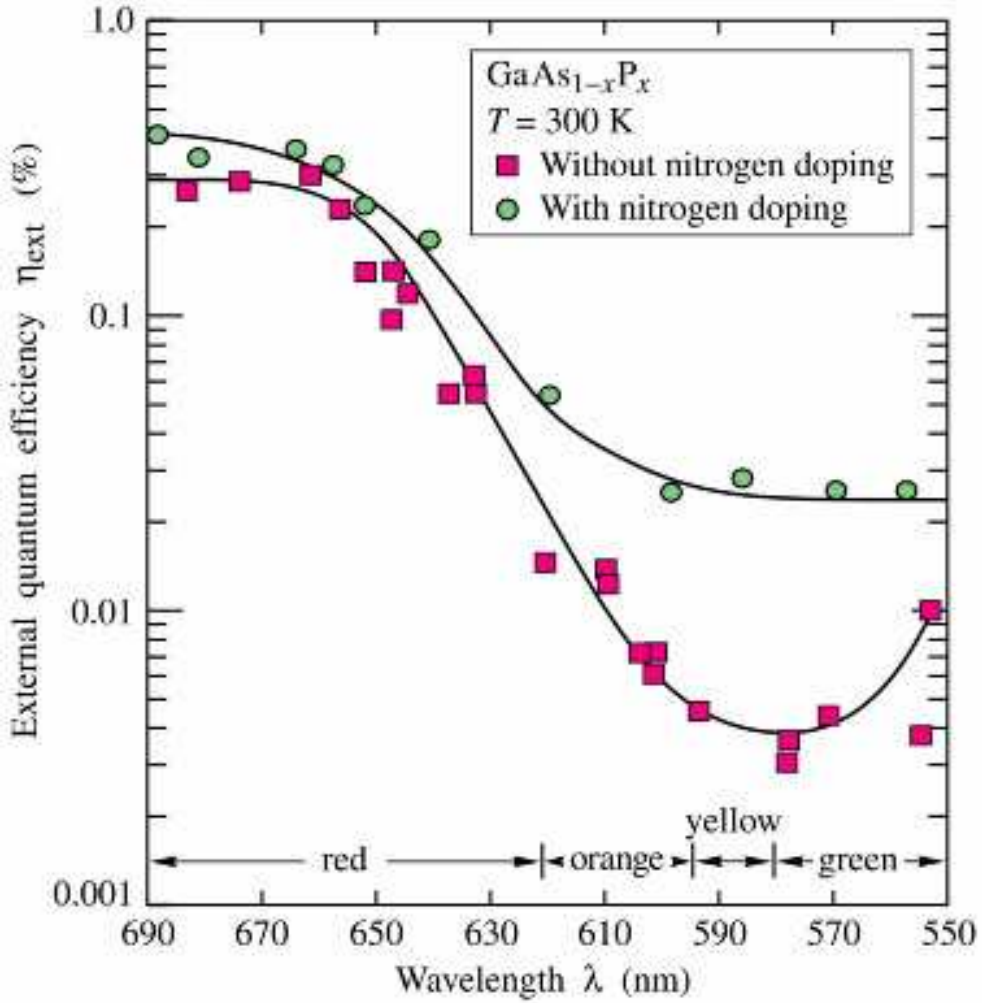

Fig. 7.4. External quantum efficiency versus emission wavelength in undoped and nitrogen-doped $GaAs_{1-x}P_x$ (after Groves *et al.*, 1978a and 1978b).

Perdidas al acoplar con una fibra η_c

Fibra con índice núcleo n_{r1}, índice 'capa' n_{r2} ($n_{r1} > n_{r2}$)

Angulo de aceptación: $\theta_a = \sin^{-1}\left(n_{r1}^2 - n_{r2}^2\right)^{1/2} = \sin^{-1}\left(A_n\right)$

A_n apertura numérica

Eficiencia de acoplo: $\eta_c = \sin^2 \theta_a$

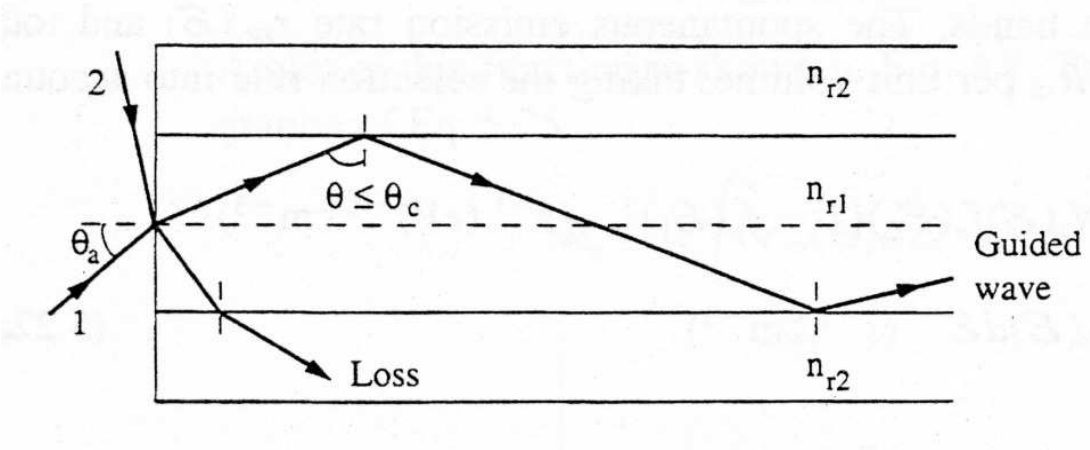

9 Estructuras: LED de heterounión

Homounión

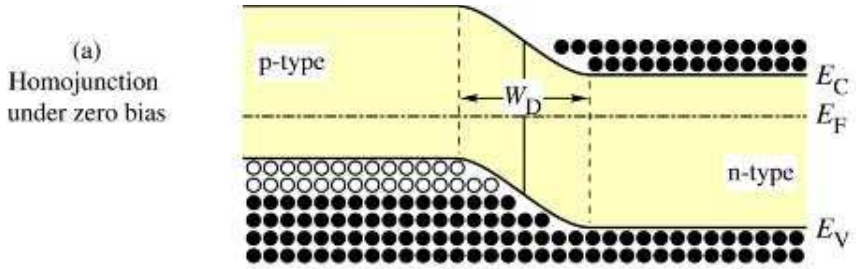

Sin Polarizar

Homounión

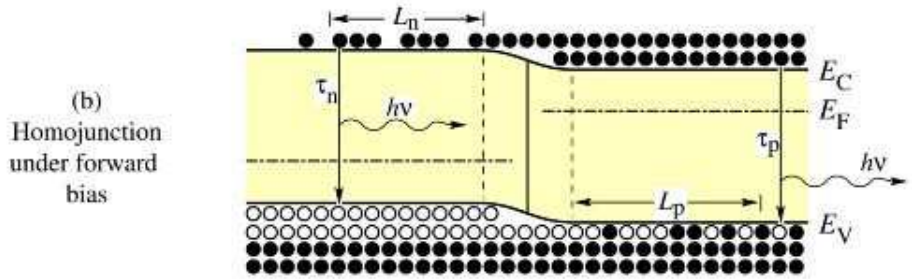

Polarización directa

Heterounión doble

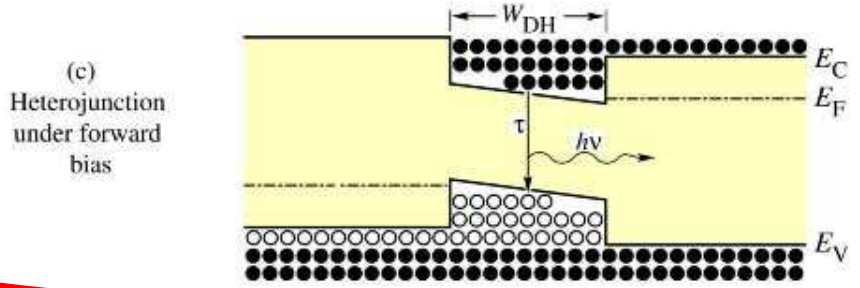

Polarización directa

Fig. 3.5. PN homojunction under (a) zero and (b) forward bias, and (c) heterojunction under forward bias. In homojunctions, carriers diffuse over the diffusion lengths L_n and L_p before recombining. In heterojunctions, carriers are confined by the heterjunction barriers.

Estructuras: LED de heterounión

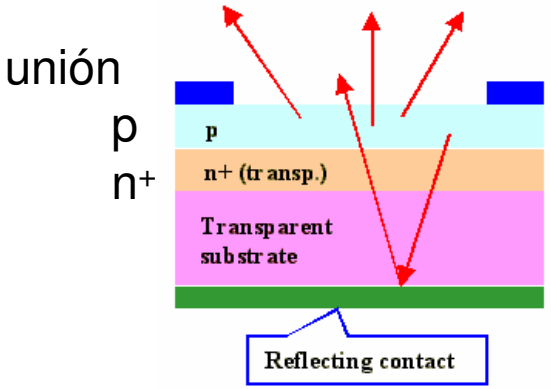

Problemas con homouniones:

1. estados de superficie en capa p cerca de la unión ⇒ recomb. no radiativa
2. electrones inyectados en capa p se alejan por difusión, recombinan con portadores mayoritarios de forma no radiativa
3. reabsorción posible

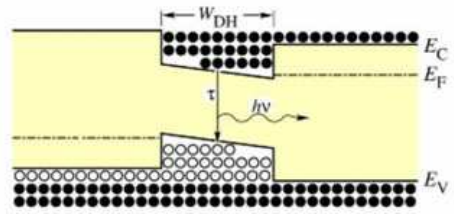

Ventajas heterounión:

1. densidad estados intercara << densidad de estados superficie
2. barrera es transparente para luz emitido (no hay reabsorción)
3. eficiencia de inyección mayor

Estructuras: LED de heterounión

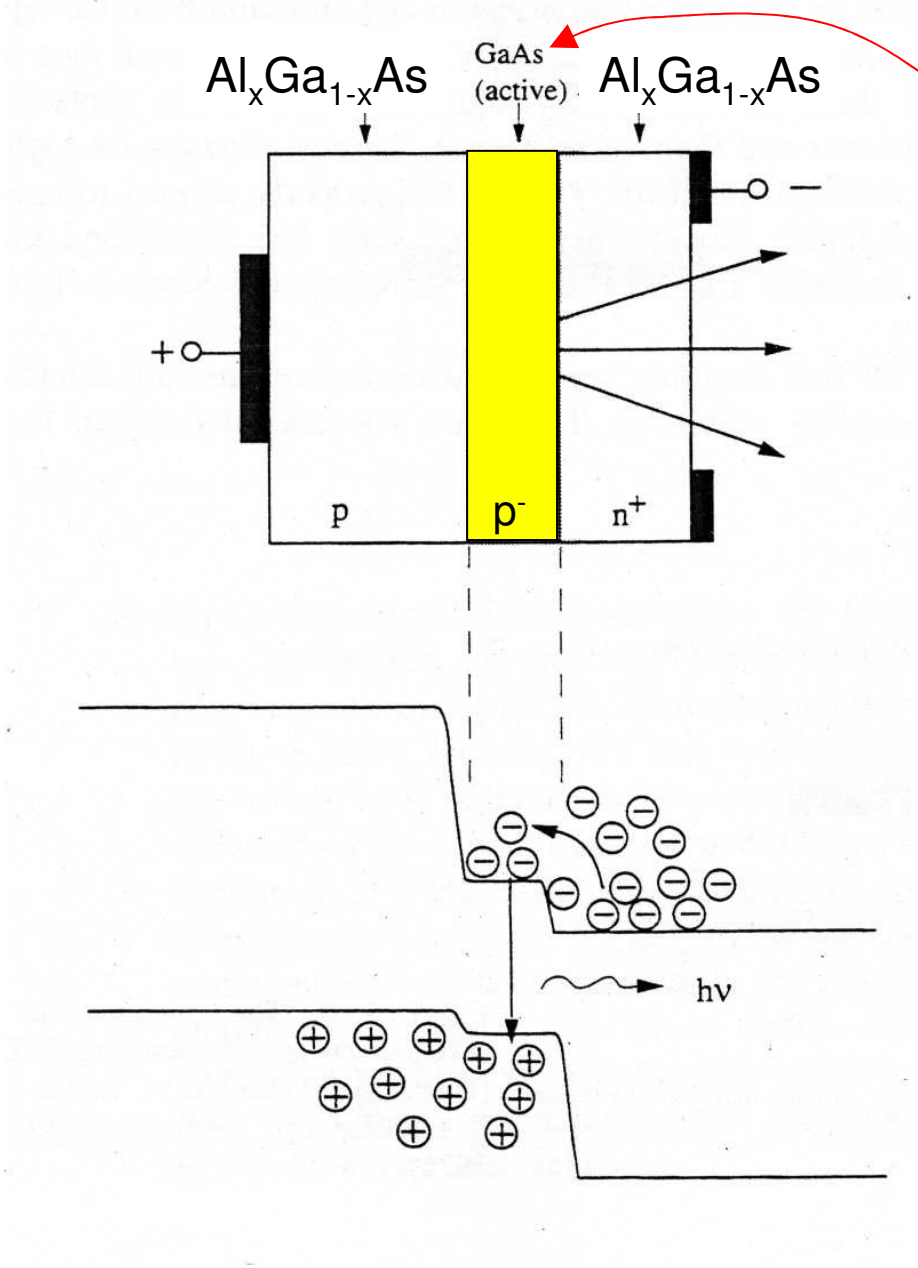

zona activa delgada
GaAs
1000 – 2000 Å

con polarización
directa

Heterounión doble: Eficiencia de Recombinación

η_r

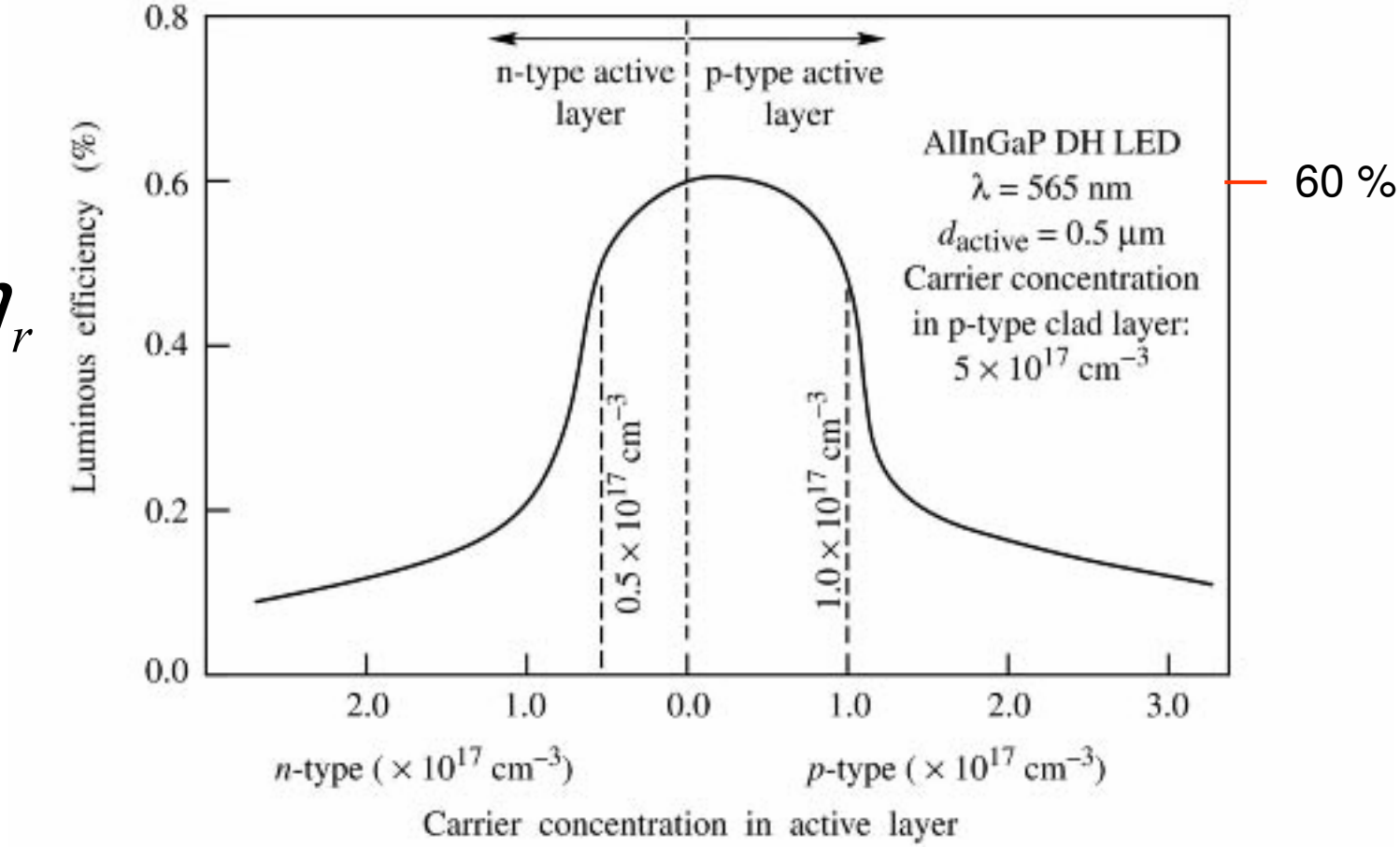

60 %

Fig. 5.4. Dependence of the luminous efficiency of an AlInGaP double heterostructure LED emitting at 565 nm on the active layer doping concentration (after Sugawara *et al.*, 1992).

Burrus Surface Emitting diode

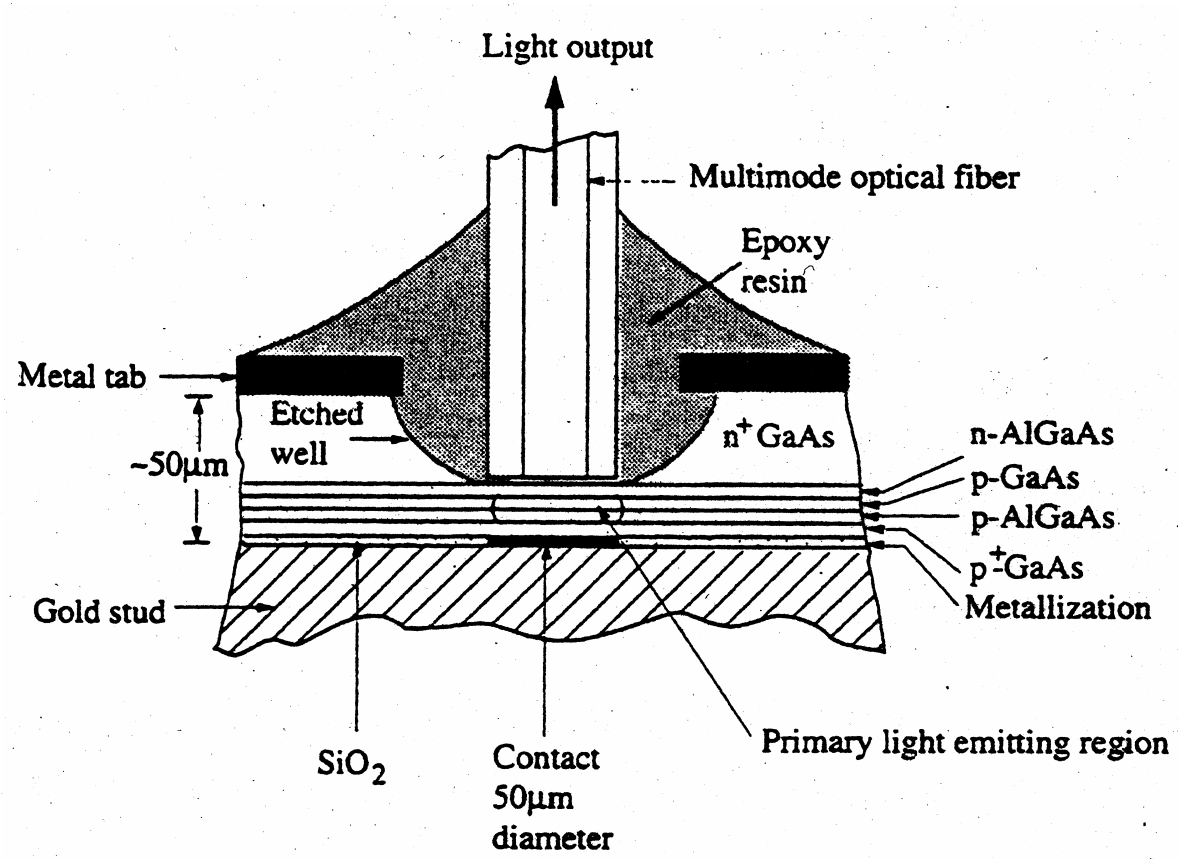

LEDs acoplados a una fibra

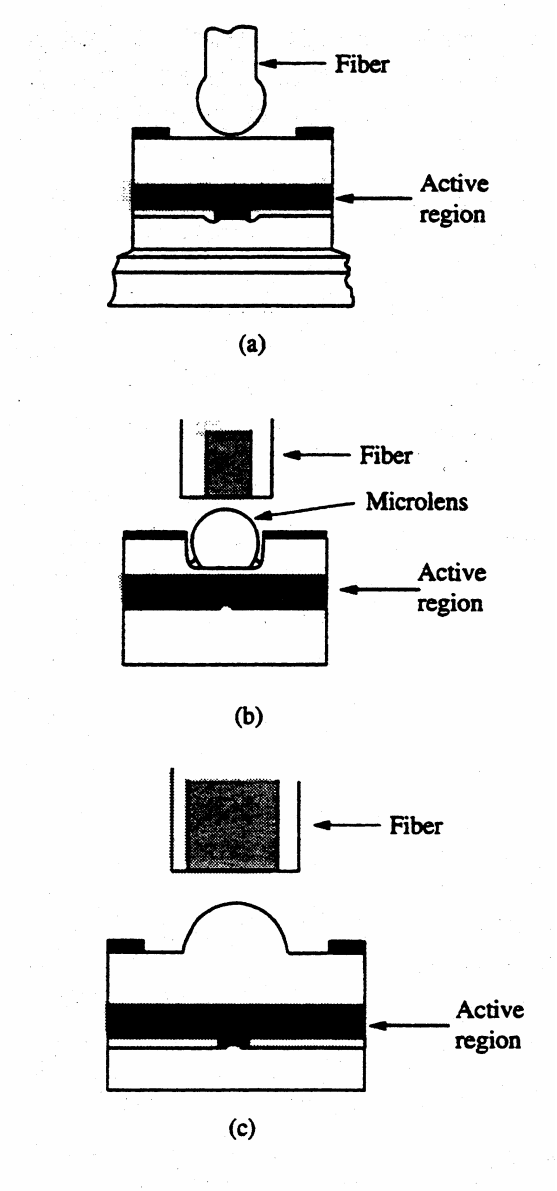

Fibra con final esférico

Microlente

Lente integrado

LEDs acoplados a una fibra

Lente integrado

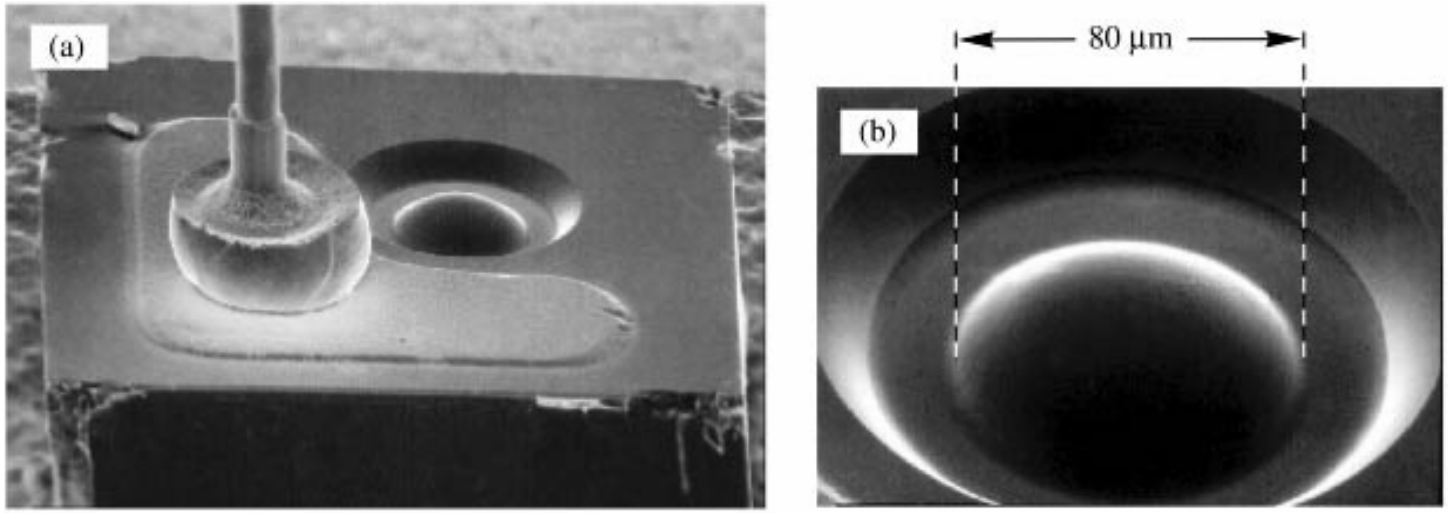

Fig. 12.8. (a) Commercial communication LED chip with integrated lens. (b) Detailed picture of the lens etched by a photochemical process into the GaAs substrate (AT&T ODL procuct line, 1995).

LED emitiendo por el borde

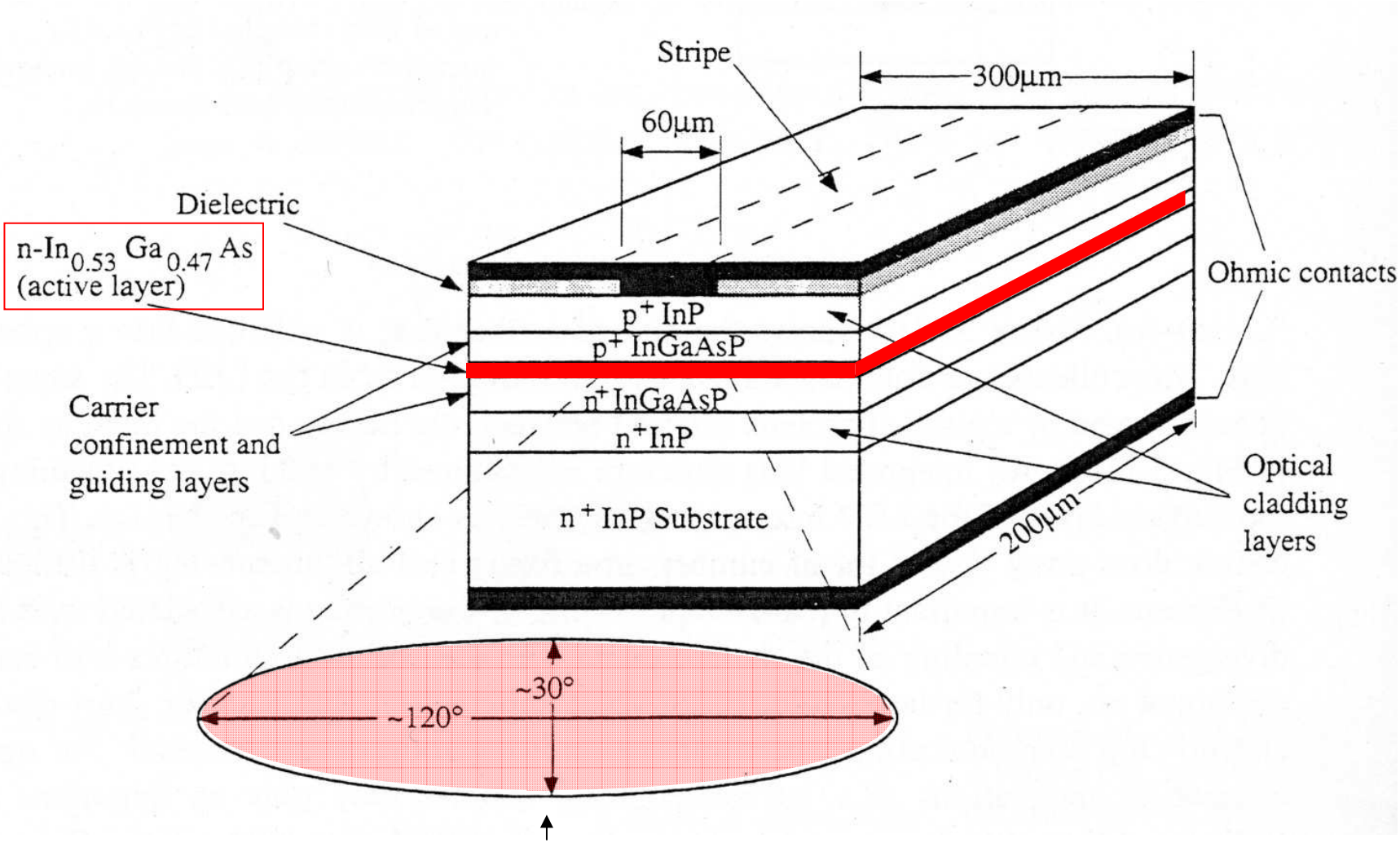

divergencia reducida

Estructuras especiales: dispersión de corriente

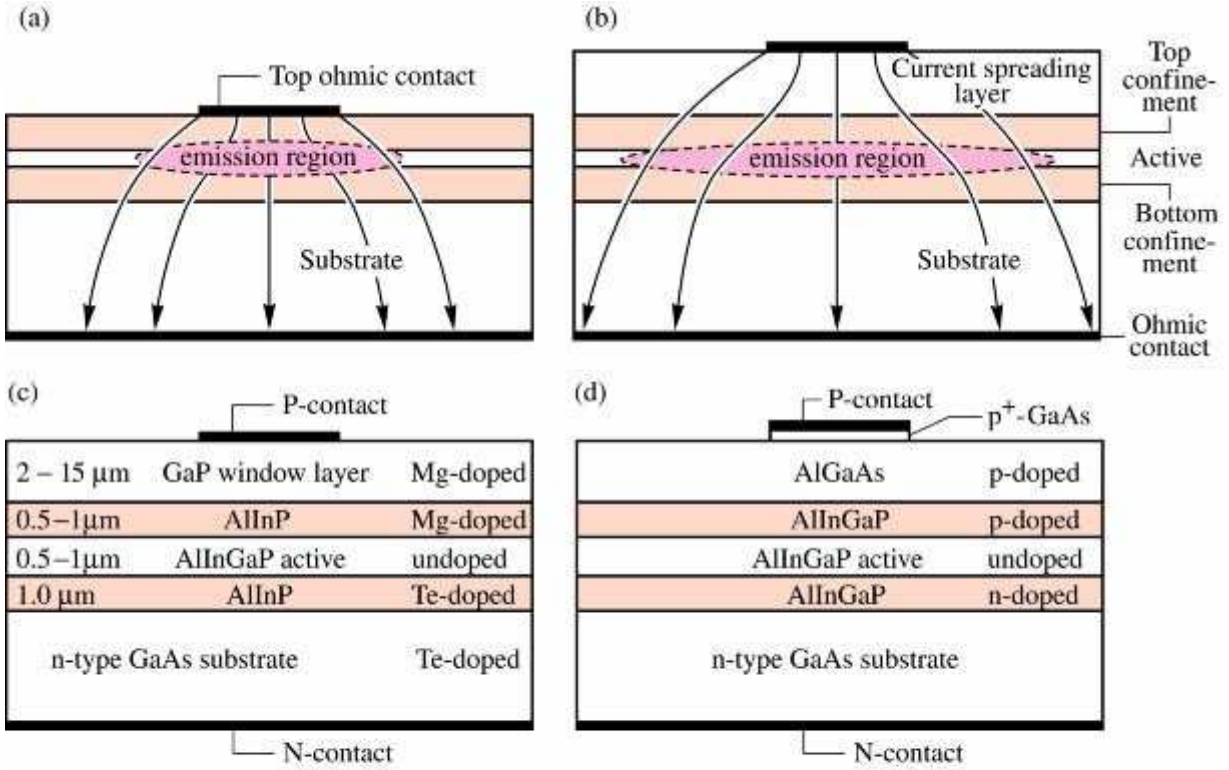

Fig. 6.8. Current spreading structures in high-brightness AlInGaP LEDs. Illustration of the effect of a current spreading layer for LEDs (a) without and (b) with a spreading layer on the light extraction efficiency. (c) GaP current spreading structure (Fletcher *et al.*, 1991). (d) AlGaAs currect spreading structure (Sugawara *et al.*,1992).

Contacto hace sombra, con capa extra sale mas luz

Estructuras especiales: sustrato transparente (TS)

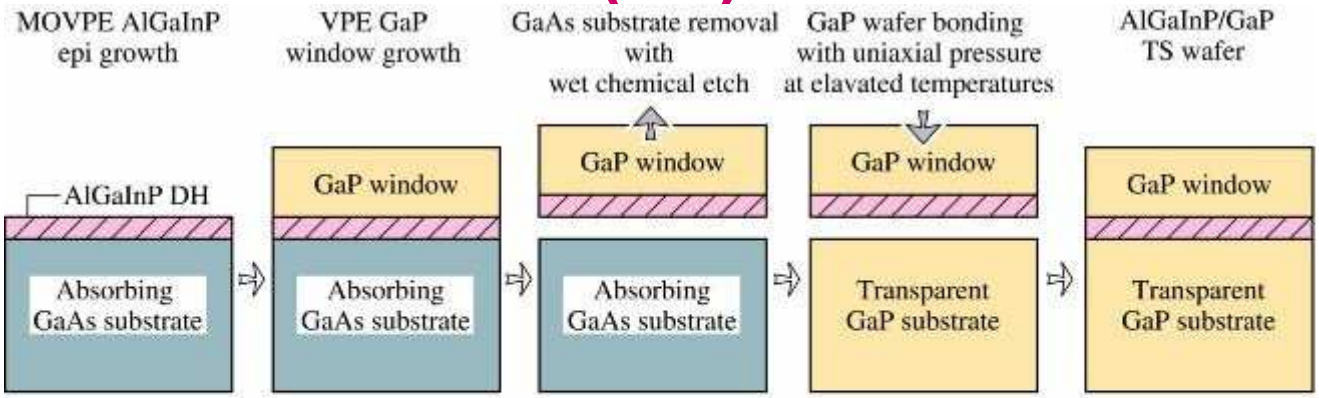

Fig. 6.14. Schematic diagram of the fabrication process for wafer-bonded tarnsparent substrate (TS) AlGaInP/GaP LEDs. After the selective removal of the original GaAs substrate, elevated temperature and uniaxial pressure are applied to the GaP substrate and the AlGaInP/GaP epitaxial film, resulting in the formation of a single TS LED wafer (adopted from Kish *et al*. 1994).

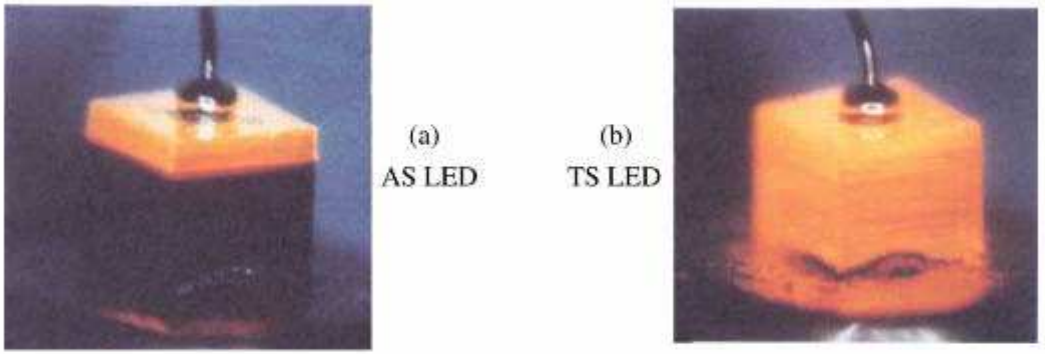

Fig. 6.15. (a) Amber GaP/AlGaInP/GaAs LED with GaP window layer and absorbing GaAs substrate (AS). (b) Amber GaP/AlGaInP/GaP LED with GaP window layer and transparent GaP substarte (TS) fabricated by a wafer bonding technique. Conductive Ag-loaded die-attach epoxy can be seen at the bottom of the TS LED (after Kish and Fletcher, 1997).

Estructuras especiales: pirámide invertida

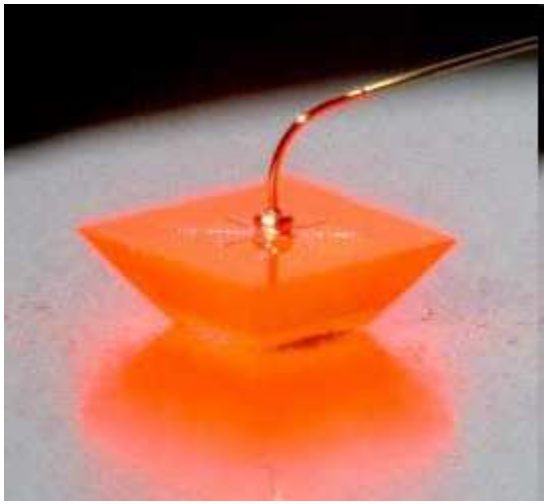

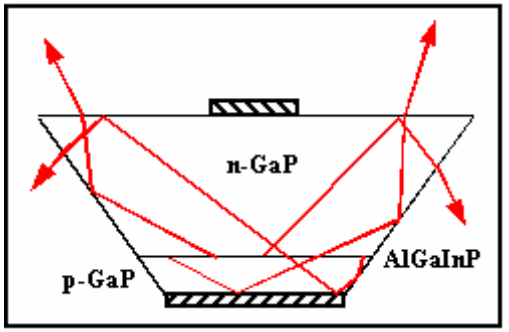

total external efficiency of 55%

10 Tiempos de respuesta

Tiempo de respuesta típica de un LED < 1 μs

- suficiente para pantallas
- crítico para uso en comunicación óptica

Factores que limitan:

1. Capacidad de la unión,
   causado por variación de la carga por V_{ext}
   (tiempo *RC*)

$$\frac{1}{C^2} = \frac{2(V_i - V_{ext})}{q\varepsilon N A^2}$$

2. Capacidad de difusión:
   La carga inyectada desaparece por difusión y recombinación
   Con modulación de V_{ext} (bias) la carga tiene que desaparecer por difusión, para adquirir nuevo equilibrio.

   $\Rightarrow$ tiempo de vida de portadores minoritarios es determinante

Tiempos de respuesta

Electrones inyectados en capa **p**

Densidad de electrones en exceso *n* disminuye por recombinación y difusión

$$\frac{\partial n(x,t)}{\partial t} = -R + D_e \frac{\partial^2 n(x,t)}{\partial x^2} \qquad R = \frac{1}{\tau} n(x)$$

Respuesta a una modulación $n(x,t) = n_0(x) + n_1(x)\exp(i\omega t)$

Respuesta del LED:

$$r(\omega) = \frac{1}{\left(1+\omega^2\tau^2\right)^{1/2}} = \frac{P(\omega)}{P(0)}$$

τ tiempo de vida de portadores minoritarios

Tiempos de respuesta / modulación

Mejor respuesta con τ pequeño, se consigue con:

1. Mayor dopaje

$$\tau = (Bn)^{-1}$$

GaAs: dopaje alto: formación de centros no-radiativos
τ = 1.4 ns

2. Dopaje bajo, zona activa pequeña, inyección alta

$$\tau \cong (B\,\Delta n)^{-1}$$

J densidad de corriente de inyección
d región activa
J/de nº de recombinaciones / $m^3 s$ = *R*

$$\Delta n = \frac{J\tau}{ed} \quad \Rightarrow \quad \tau = \left(\frac{ed}{JB}\right)^{1/2}$$

Tiempos de respuesta / modulación

Formulación alternativa:

anchura de banda : frecuencia a la cual *P* disminuye 3dB

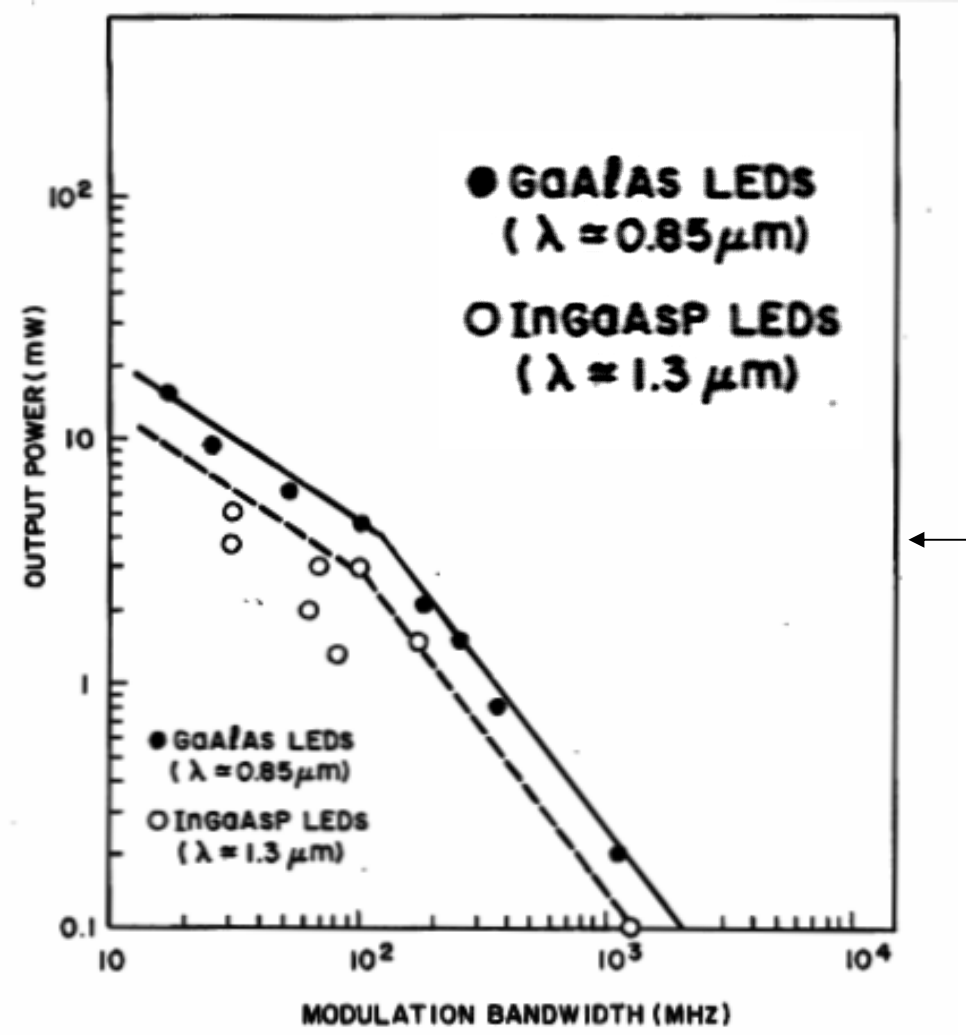

← Potencia de salida en función de la modulación

MHz

11 Circuitos

DC

AC

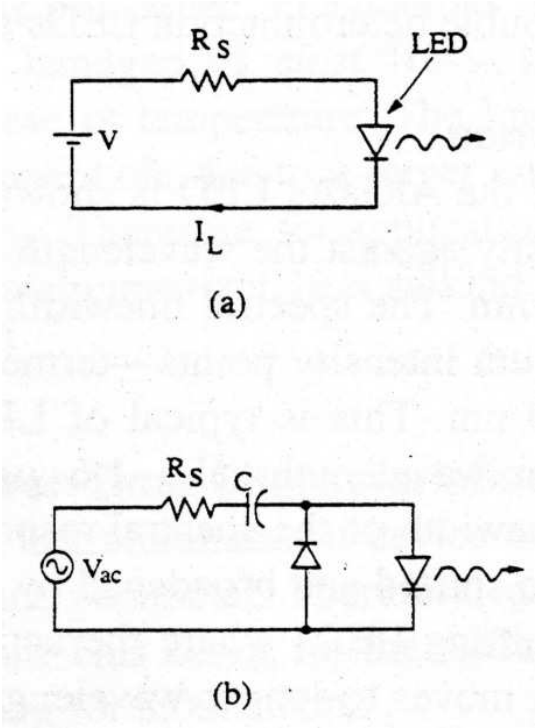

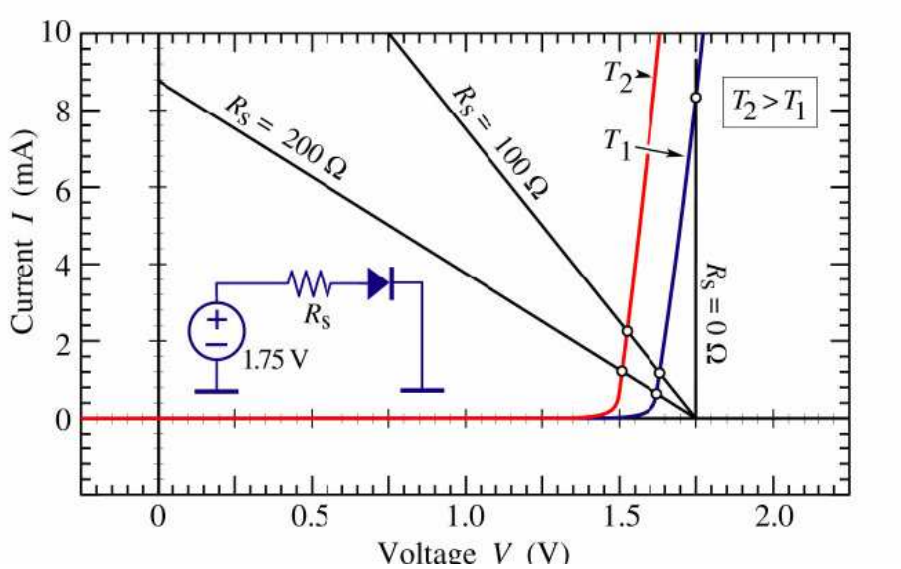

I ~ 20 – 100 mA

$V_{directa}$ 1.2 V (GaAs)

2 V (GaP)

Circuito para modulación

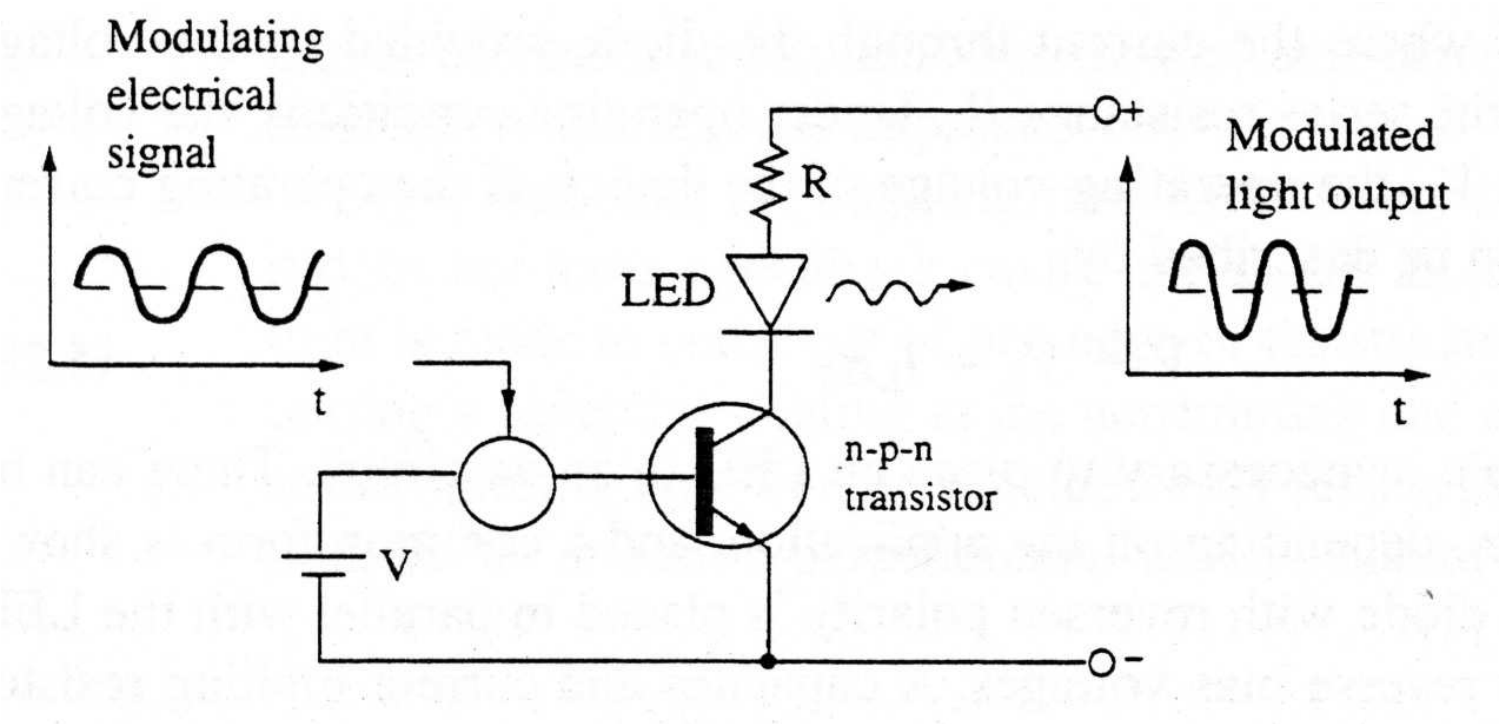

12 LED en cavidad resonante (RCLED)

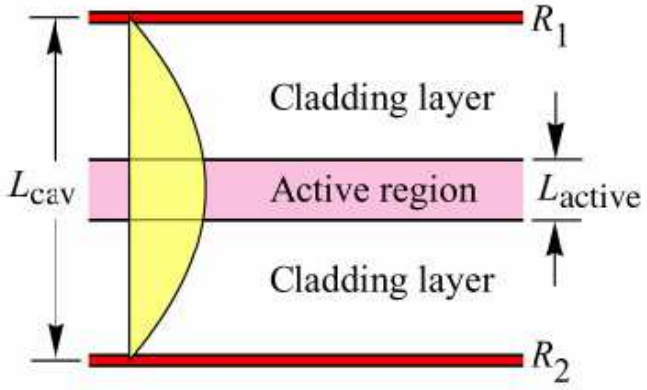

Fig. 10.1. Schematic illustration of resonant cavity consisting of two metal mirrors with reflectivity R_1 and R_2. The active region has a thickness L_{active} and an absorption coefficient α. Also shown is the standing optical wave. The cavity length is L_{cav} is equal to $\lambda / 2$.

RCLED - modos en una cavidad

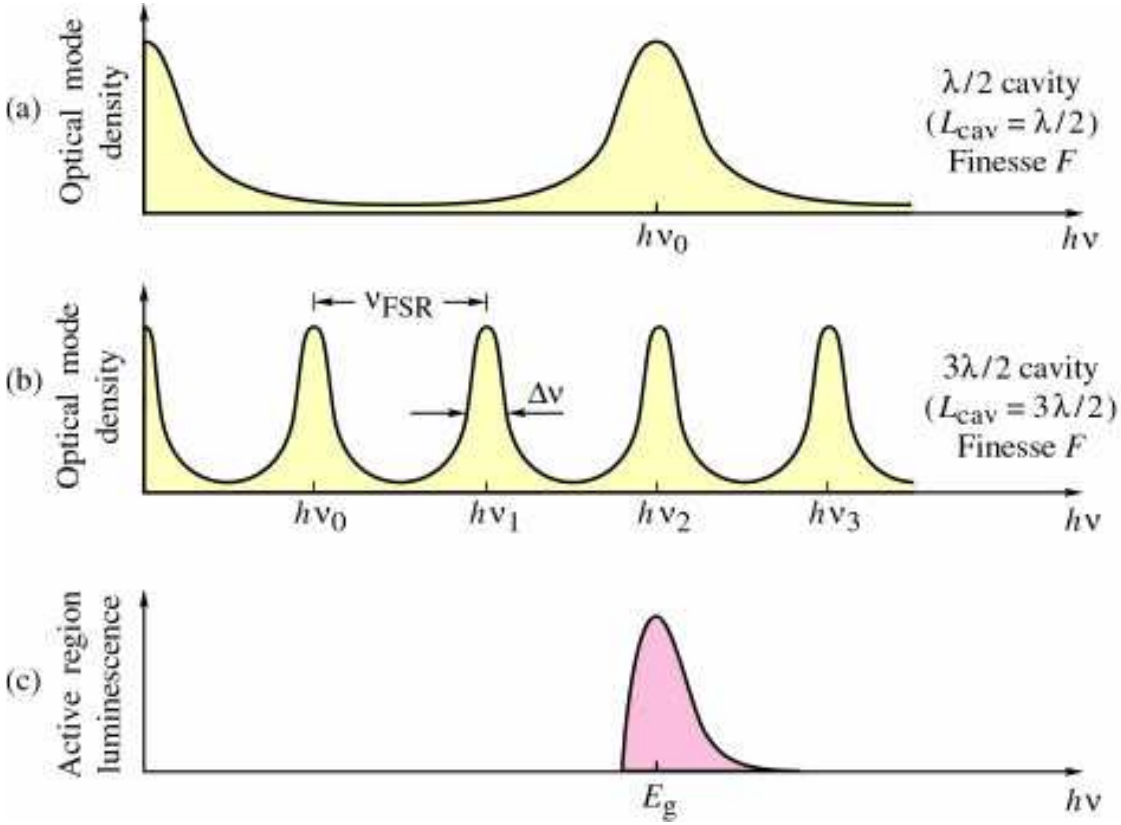

Fig. 9.2. Optical mode density for a (a) short and (b) long cavity with the same finesse F. (c) Spontaneous free space emission spectrum of an LED active region. The spontaneous emission spectrum has a better overlap with the short-cavity mode-spectrum as compared to the long-cavity mode-spectrum.

Solape de la emisión espontánea con modo de cavidad

Distributed Bragg Reflector (DBR)

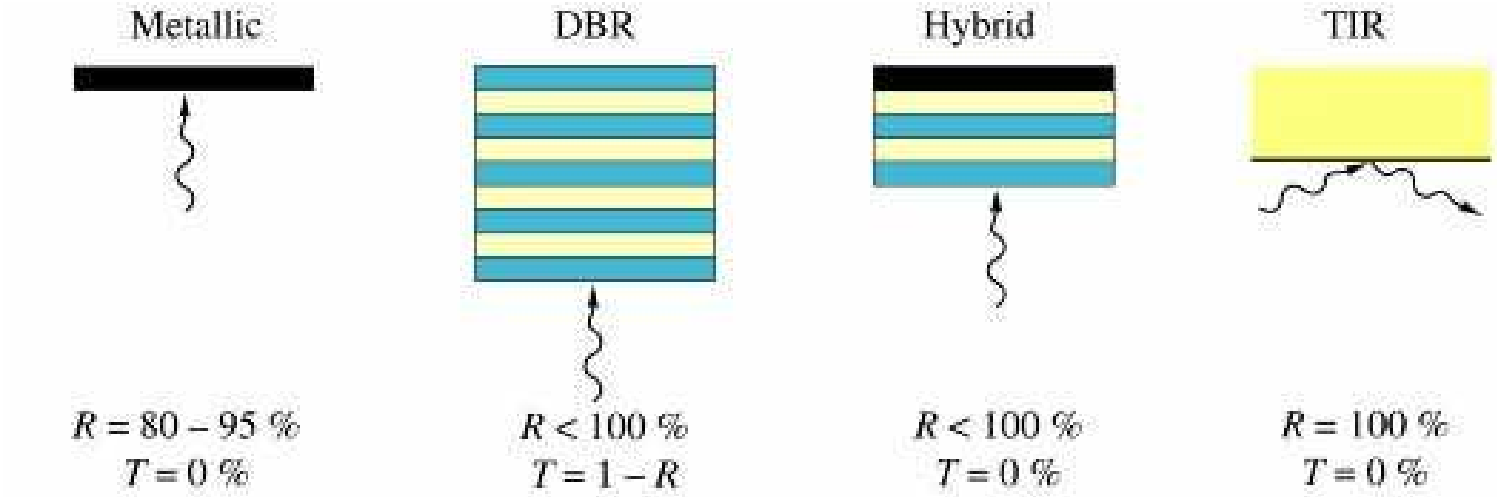

Fig. 8.3. Schematic illustration of different types of reflectors including metallic reflector, distributed Bragg reflector (DBR), hybrid reflector, and total internal reflector (TIR).

Distributed Bragg Reflector (DBR)

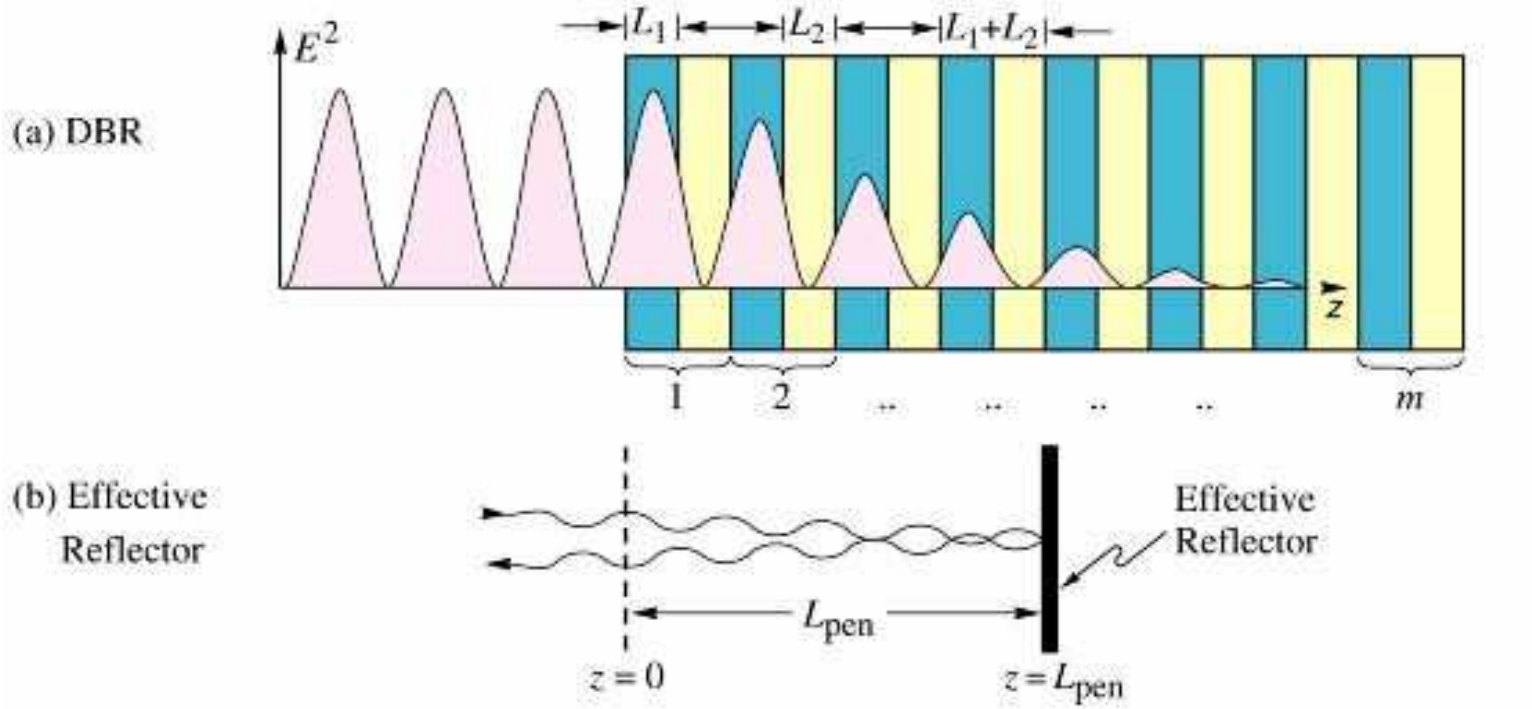

Fig. 8.5. Illustration of the DBR penetration depth. (a) DBR consisting of two materials with thickness L_1 and L_2. (b) Ideal (metallic) reflector displaced from the DBR surface by the penetration depth.

Distributed Bragg Reflector (DBR)

Reflector aire/Plata

DBR

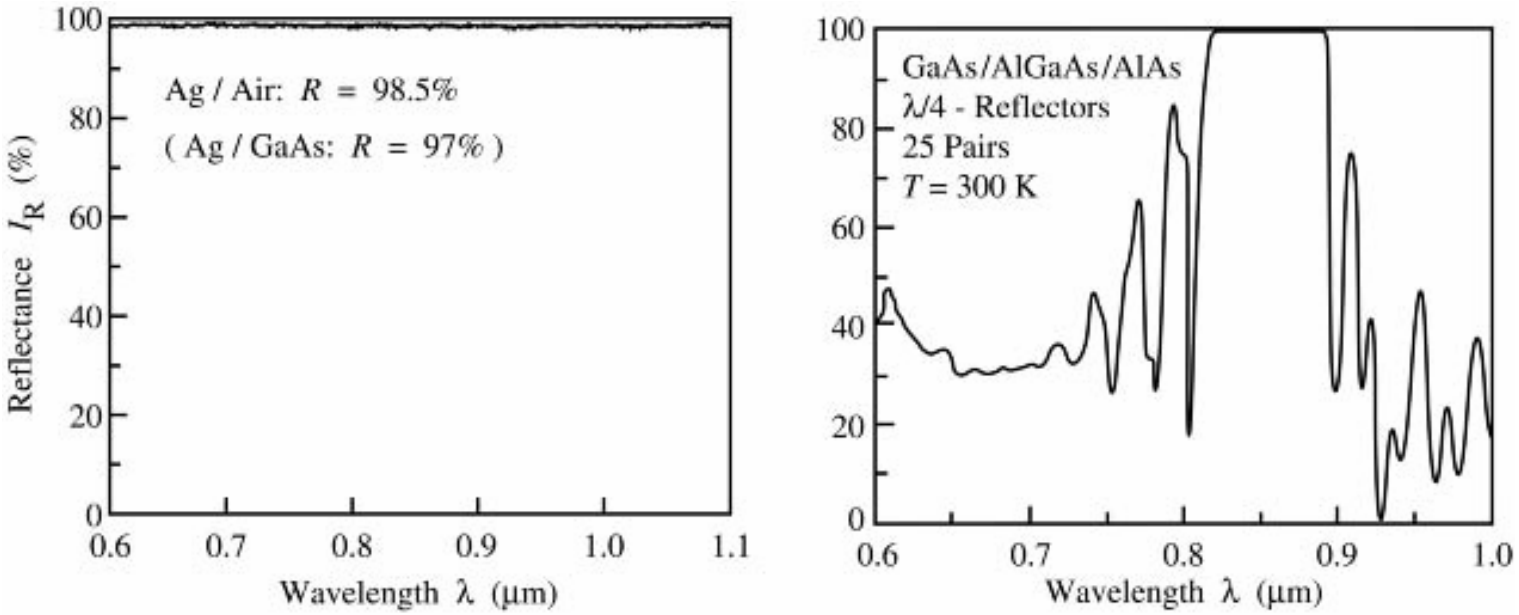

Fig. 8.4. Reflectance of a silver / air reflector and a 25-pair AlAs / GaAs distributed Bragg reflector (DBR).

RCLED vs. VCSEL

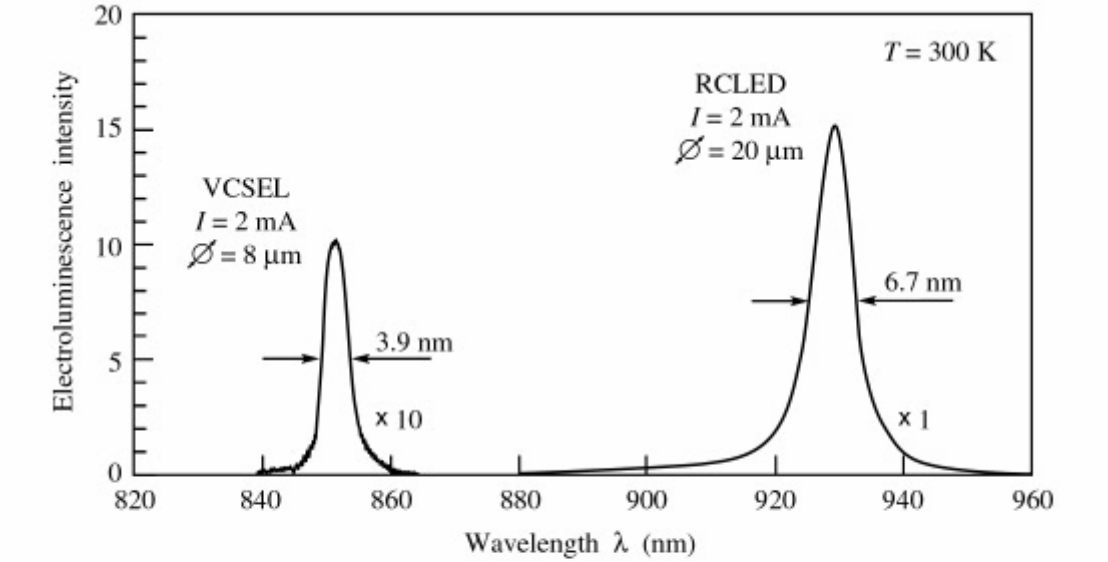

Fig. 9.3. Spontaneous electroluminescence spectrum of a vertical-cavity surface-emitting laser (VCSEL) emitting at 850 nm and of a resonant-cavity light-emitting diode (RCLED) emitting at 930 nm. The drive current for both devices is 2 mA. The VCSEL spectrum is multiplied by a factor of ten. The threshold current of the VCSEL is 7 mA.

VCSEL (Vertical Cavity Surface Emitting Laser) tiene menos intensidad en régimen de emisión espontánea

RCLED

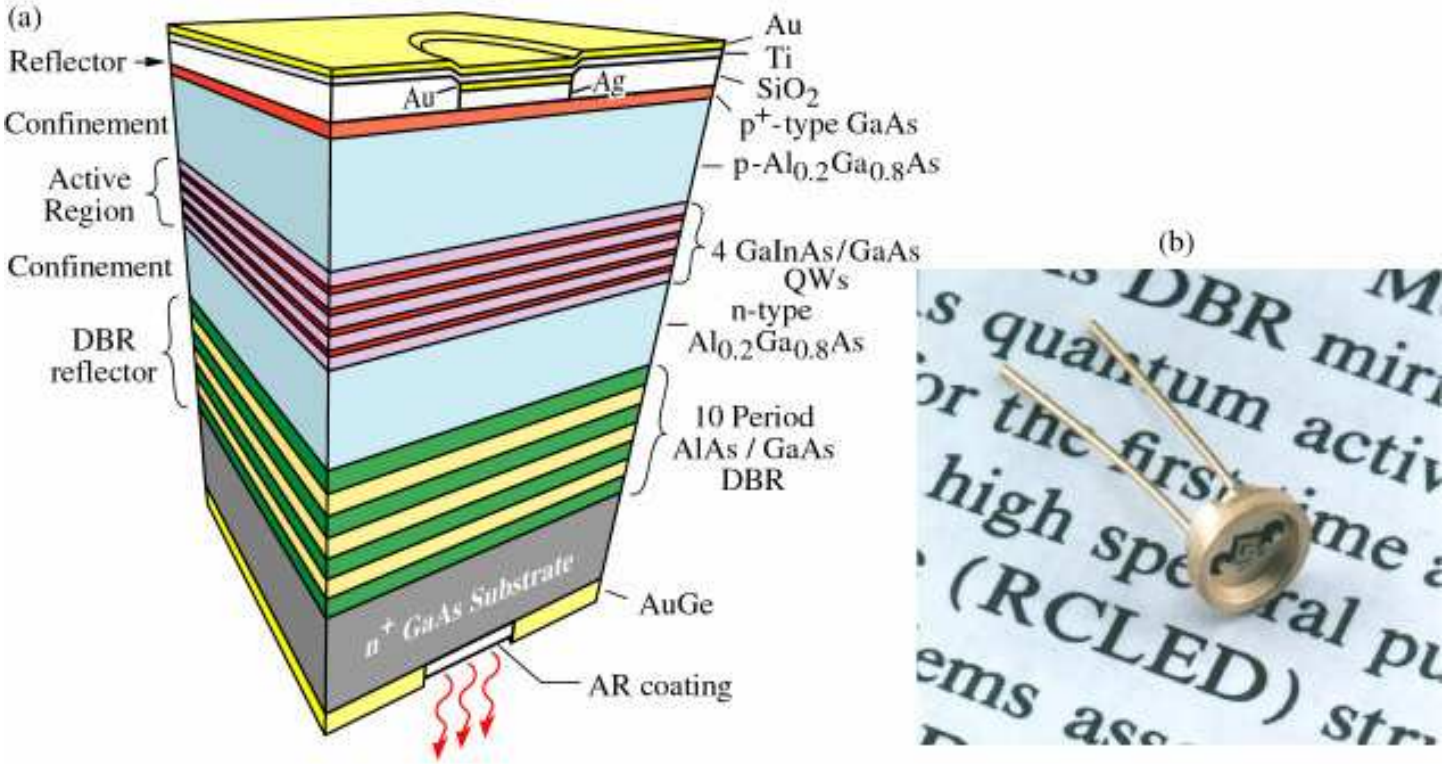

Fig. 9.4. (a) Schematic structure of a substrate-emitting GaInAs / GaAs RCLED consisting of a metal top reflector and a bottom distributed Bragg reflector (DBR). The RCLED emits at 930 nm. The reflectors are an AlAs / GaAs DBR and a Ag top reflector (after Schubert *et al.*, 1994). (b) Picture of the first RCLED.

RCLED espectro de emisión

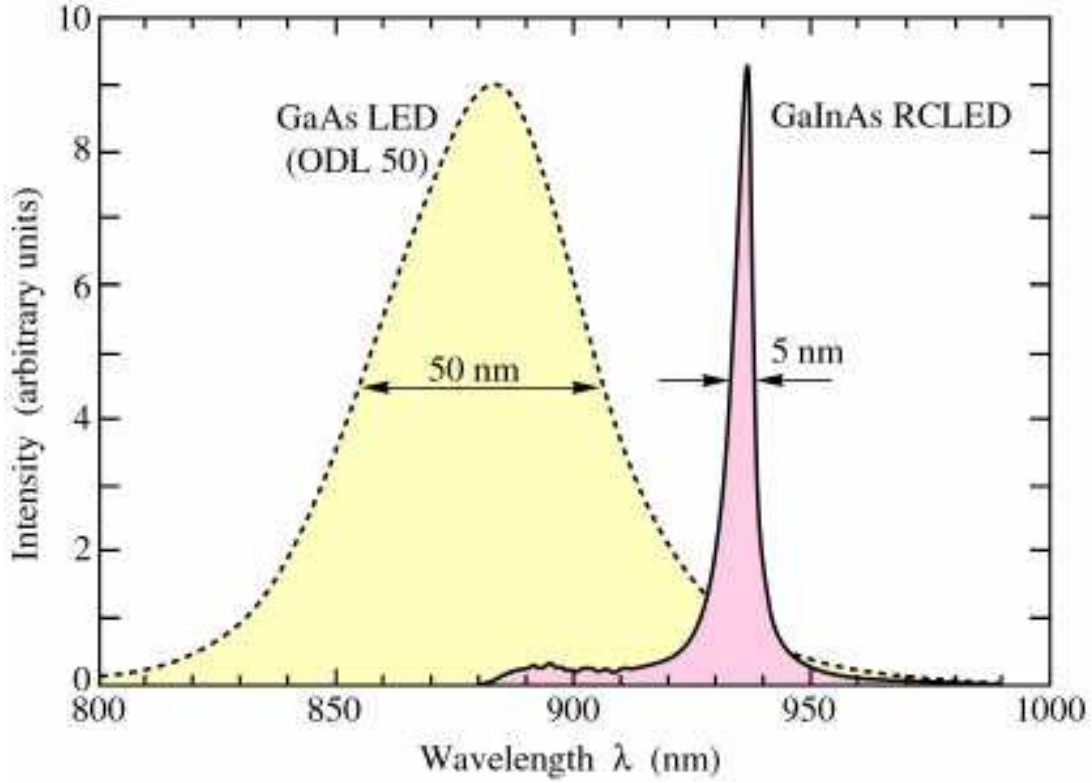

Fig. 9.6. Comparison of the emission spectra of a GaAs LED emitting at 870 nm (AT&T ODL 50 product) and a GaInAs RCLED emitting at 930 nm.

13 Visión humana: sensibilidad del ojo

Función de la sensibilidad del ojo humano $V(\lambda)$

Definición del lumen:
Luz verde (555 nm) de 1 W tiene un flujo luminoso de 683 lm

$$\ln[V(\lambda)] = A_0 + A_1\lambda^1 + A_2\lambda^2 + A_3\lambda^3 + A_4\lambda^4 + A_5\lambda^5$$

$380\ \text{nm} \le \lambda \le 520\ \text{nm}$: $A_0 = -502.77$, $A_1 = -1.3992$, $A_2 = 0.0336$, $A_3 = -0.0001$
$A_4 = 2.0 \times 10^{-7}$, $A_5 = -1.0 \times 10^{-10}$ $(R^2 = 0.9988)$

$520\ \text{nm} \le \lambda \le 750\ \text{nm}$: $A_0 = 1072.6$, $A_1 = -8.7481$, $A_2 = 0.0276$, $A_3 = -4.0 \times 10^{-5}$
$A_4 = 3.0 \times 10^{-8}$, $A_5 = -9.0 \times 10^{-12}$ $(R^2 = 0.9998)$

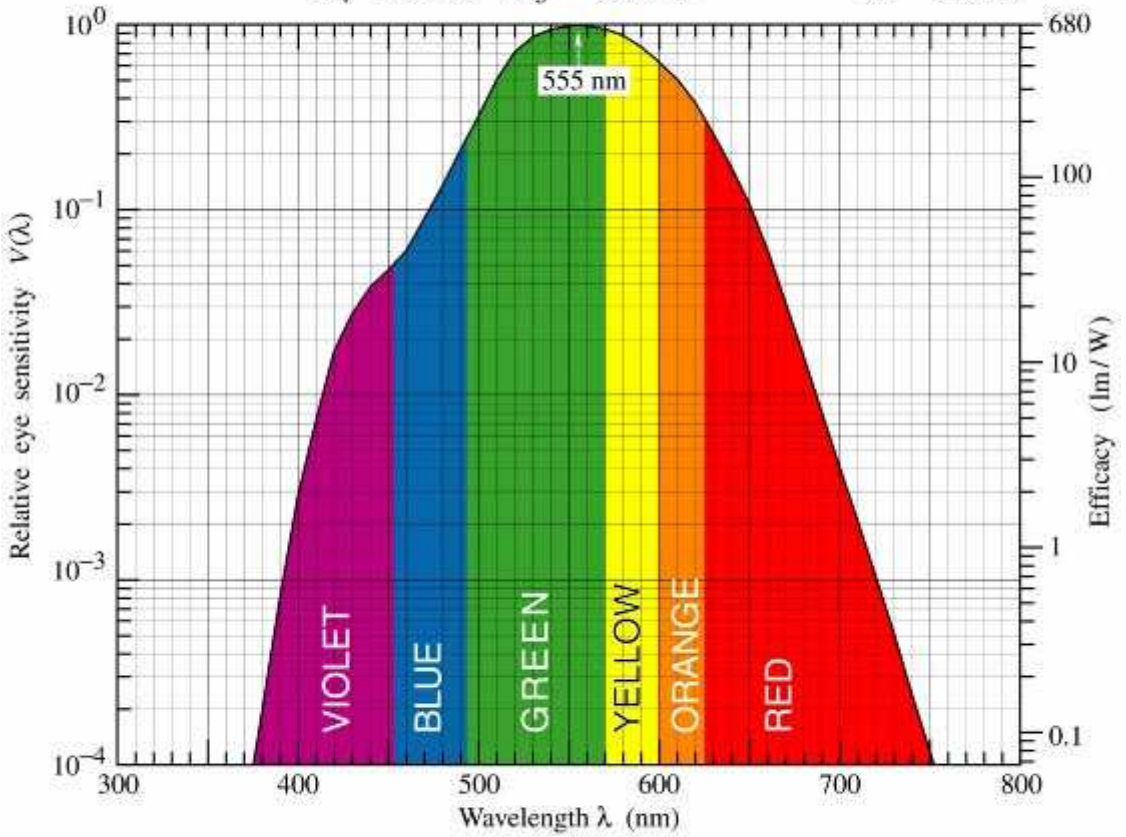

Fig. 10.1. Relative eye sensitivity (left ordinate) and efficacy measured in lumens per Watt of optical power (right ordinate). The eye sensitivity is most sensitive at 555 nm. Also given is a polynomial approximation for the relative eye sensitivity function.

Visión humana

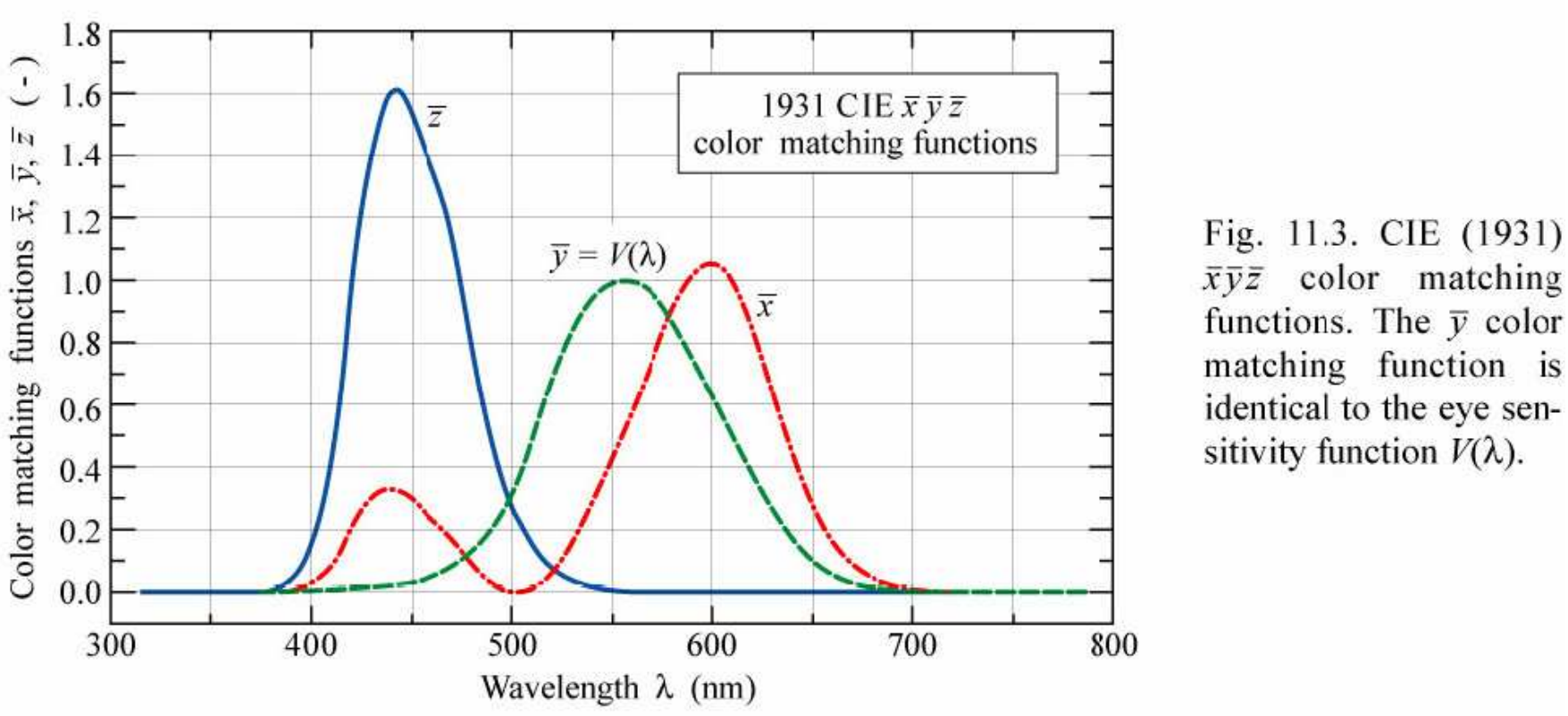

Fig. 11.3. CIE (1931) $\bar{x}\bar{y}\bar{z}$ color matching functions. The $\bar{y}$ color matching function is identical to the eye sensitivity function $V(\lambda)$.

Las funciones son similar a la sensibilidad espectral de los conos en el ojo

Visión humana

$$X = \int_{\lambda} \bar{x}(\lambda)\, P(\lambda)\, d\lambda$$

$$Y = \int_{\lambda} \bar{y}(\lambda)\, P(\lambda)\, d\lambda$$

$$Z = \int_{\lambda} \bar{z}(\lambda)\, P(\lambda)\, d\lambda$$

X, *Y*, and *Z* are ***tristimulus values***

Chromaticity diagram and ***chromaticity coordinates*** *x*, *y*

$$x = \frac{X}{X + Y + Z} \qquad y = \frac{Y}{X + Y + Z}$$

z chromaticity coordinate not needed, since $x + y + z = 1$

Uniform chromaticity coordinates *u*, *v* and *u'*, *v'*

Visión humana

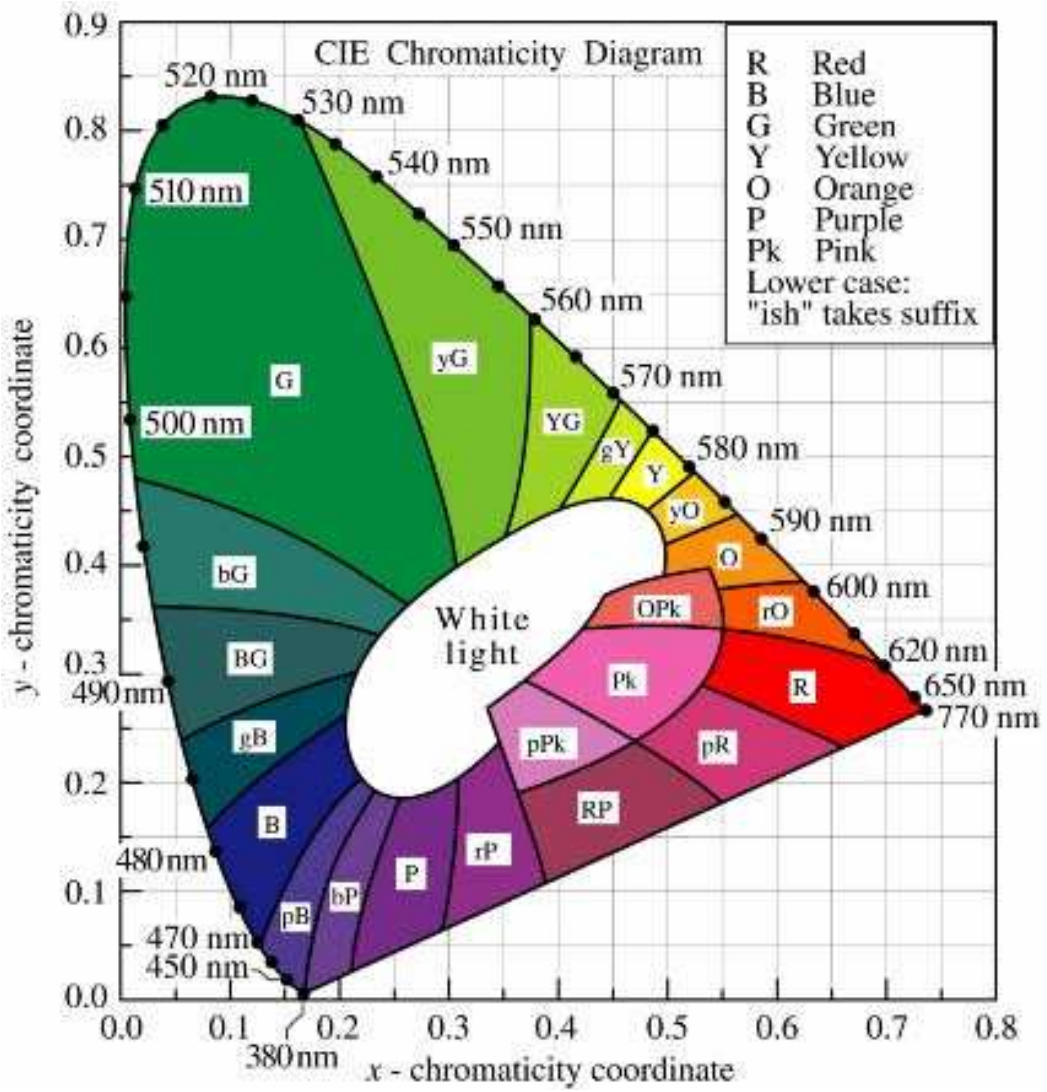

Fig. 10.3. CIE chromaticity diagram. Monochromatic colors are located on the perimeter and white light is located in the center of the diagram (adopted from Gage *et al.*, 1977).

Mezclar colores

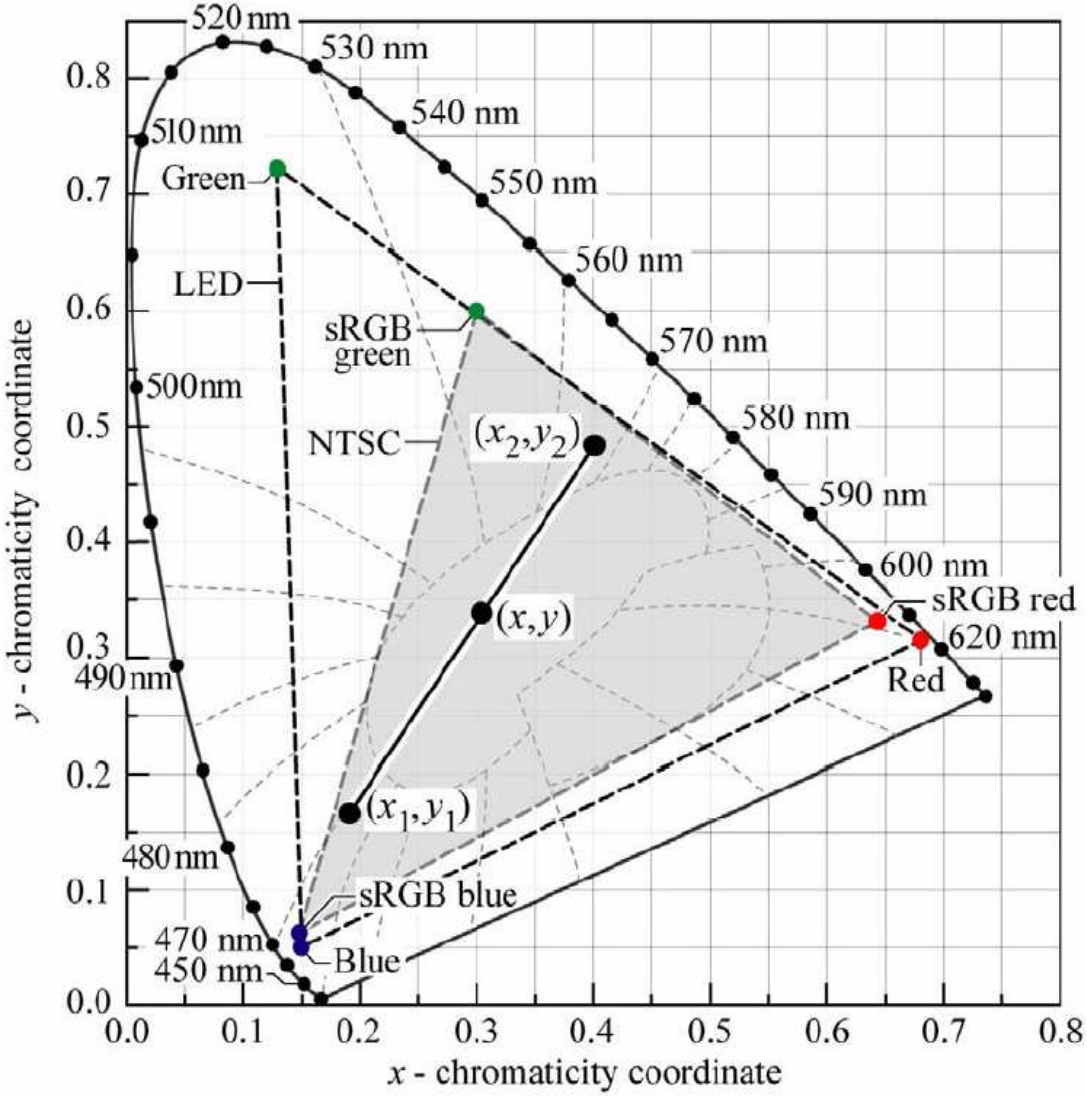

Fig. 11C.1. Principle of color mixing illustrated with two light sources with chromaticity coordinates (x_1, y_1) and (x_2, y_2). The resulting color has the coordinates (x, y). Also shown is the triangular area of the chromaticity diagram (color gamut) accessible by additive mixing of a red, green, and blue LED. The locations of the red, green, and blue phosphors of the sRGB display standard ($x_r = 0.64$, $y_r = 0.33$, $x_g = 0.30$, $y_g = 0.60$, $x_b = 0.15$, $y_b = 0.06$) are also shown. The sRGB standard is similar to the NTSC standard.

Visión humana y LEDs

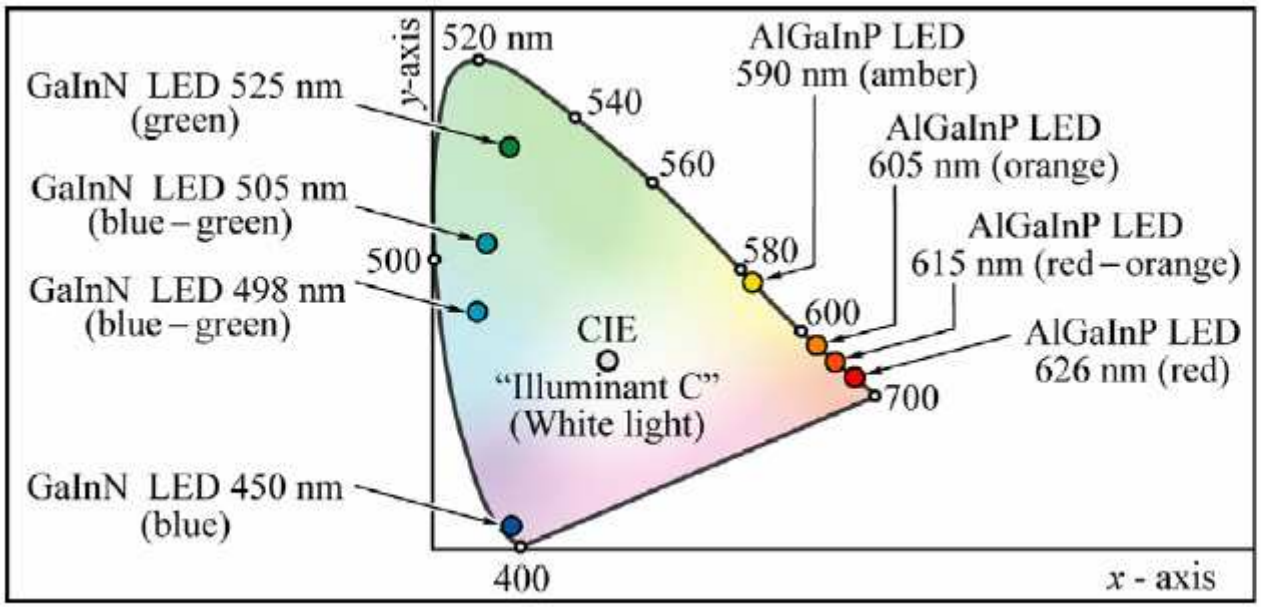

Fig. 11B.9. Location of LED light emission on the chromaticity diagram (adopted from Schubert and Miller, 1999).

14 LEDs con luz blanca

LED de InGaN emitiendo azul con un fósforo emitiendo en amarillo

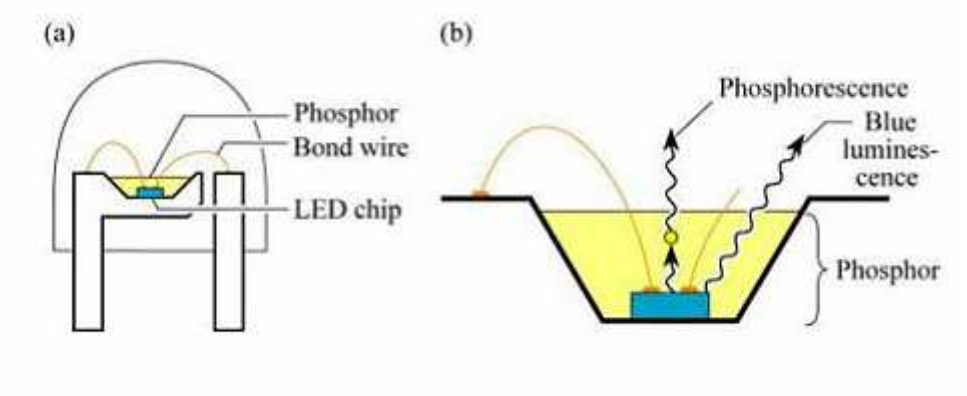

primer diseño

diseño sobre un solo chip

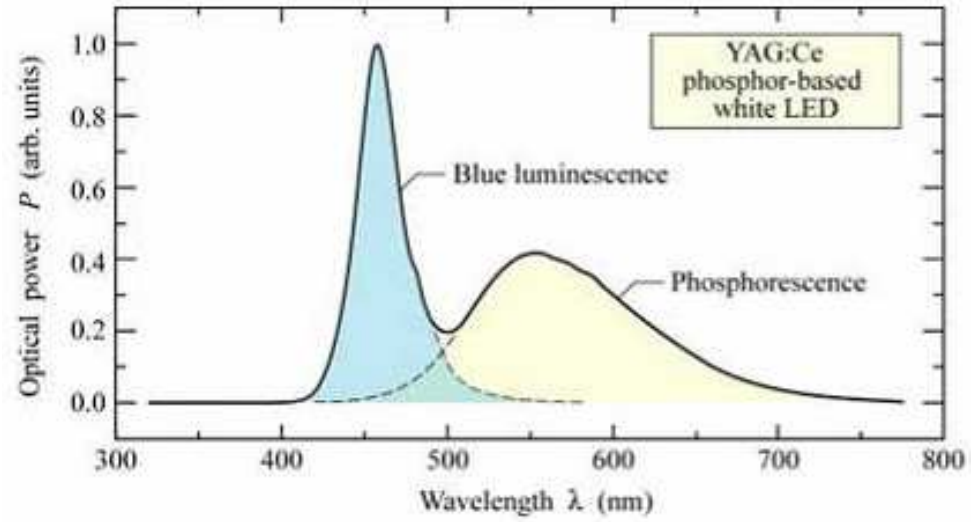

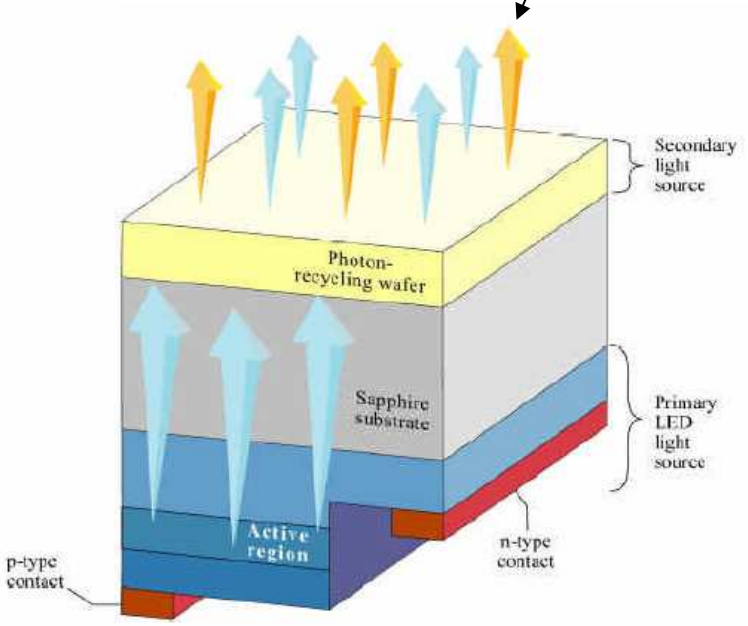

Luz blanca con LEDs

- **Direct – RGB LEDs**
  - Potentially highest efficiency
  - Very large color gamut
  - Tunable white point
- **Blue LED + yellow phosphor**
  - Simple
  - Decent color rendering (R_a ~75)
- **UV LED + RGB phosphors**
  - White point determined by phosphors only
  - Excellent color rendering

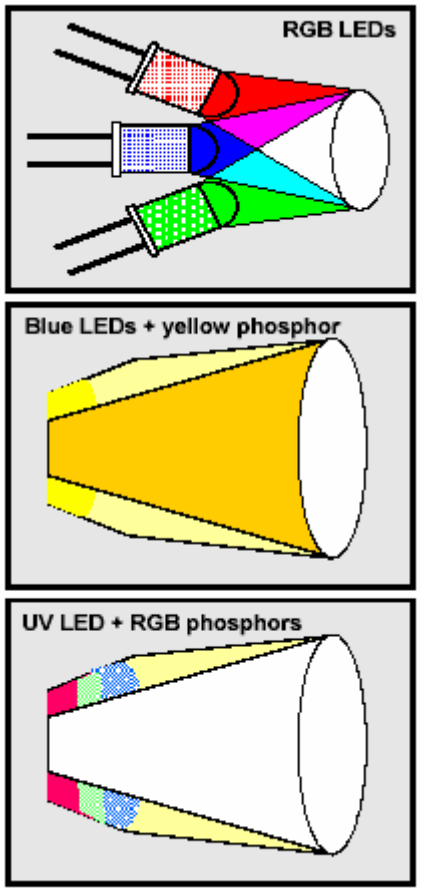

LED para iluminación

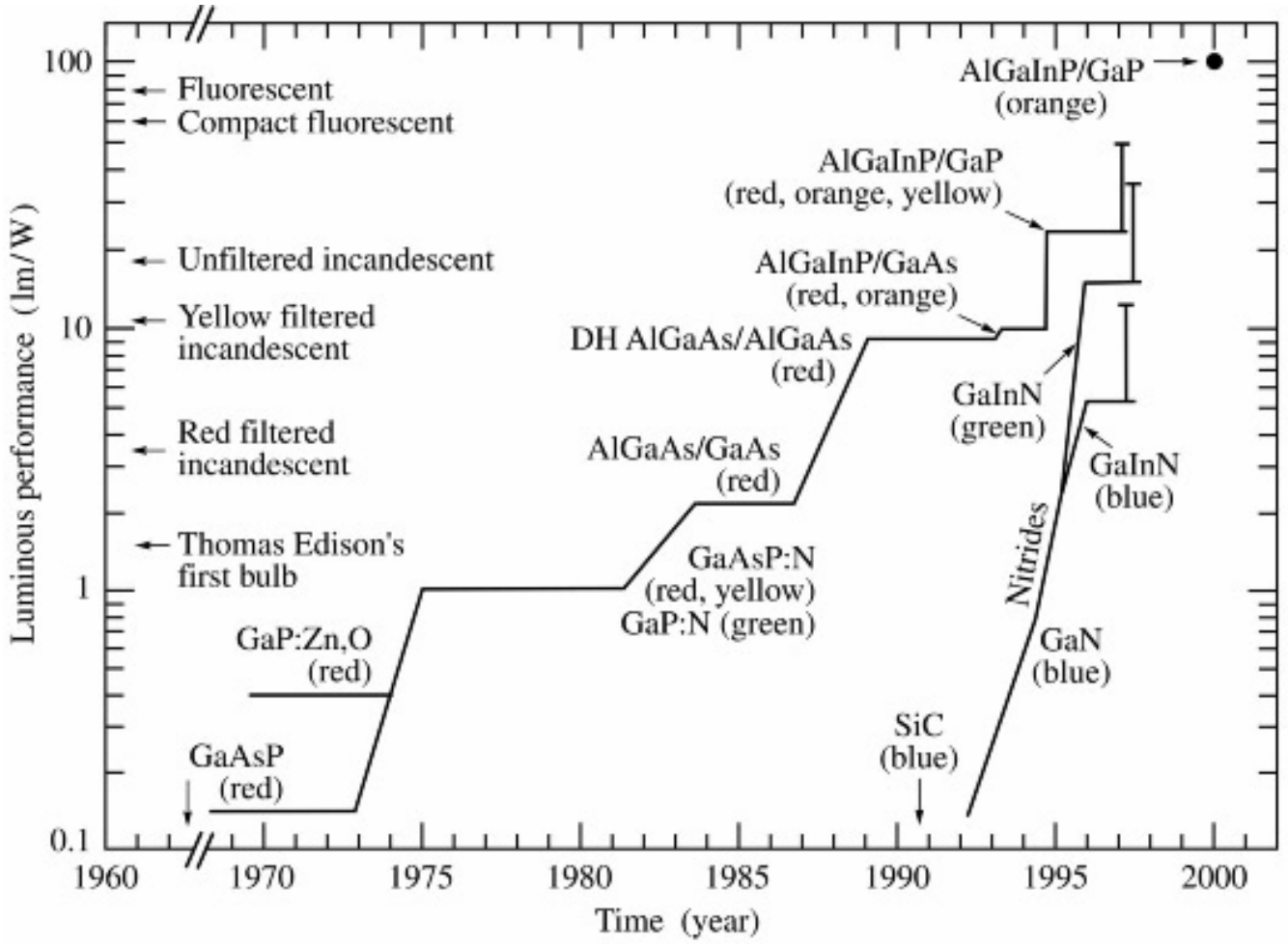

Fig. 7.13. Luminous performance of visible LEDs versus time. Also shown is the luminous performance to other light sources (adopted from Craford, 1997, 1999, updated 2000).

LED para iluminación

Flujo luminoso

Precio

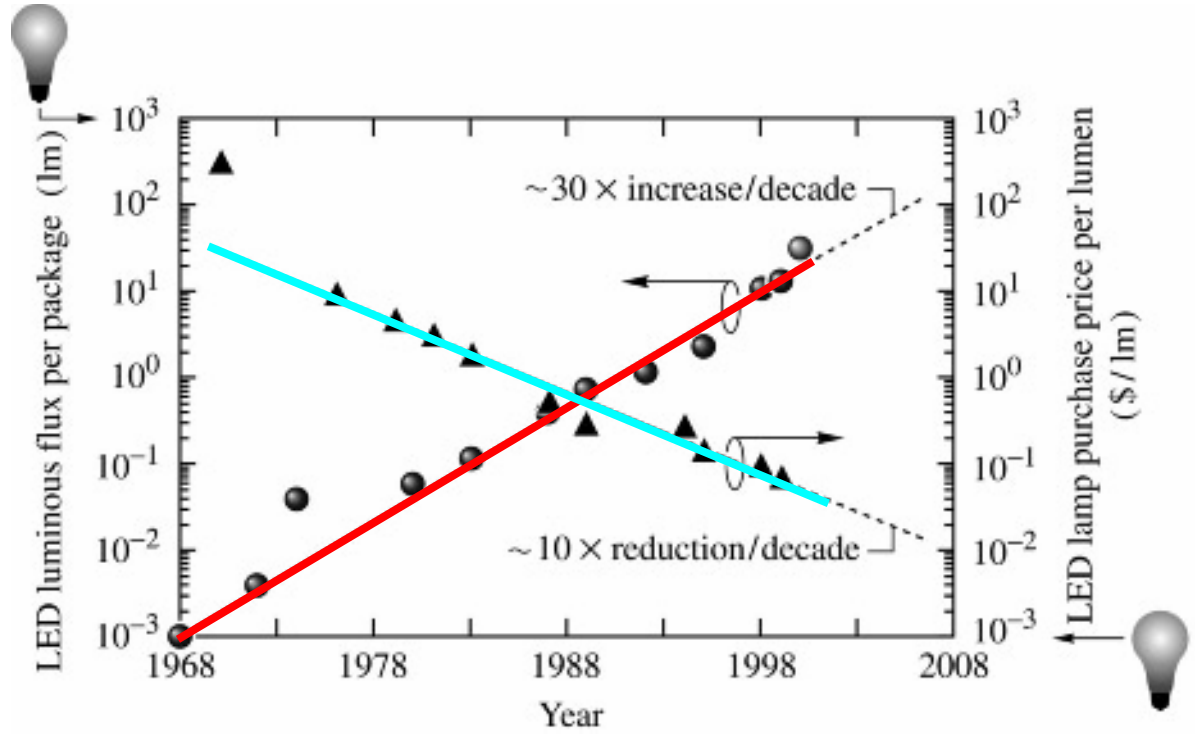

Fig. 7.15. LED luminous flux per package and LED lamp purchase price per lumen versus year. Also shown are the values for a 60 W incandescent tungsten-filament light bulb with a luminous performance of about 17 lm/W and a luminous flux of 1000 lm with an approximate price of US $ 1.00 (after Krames *et al.*, 2000).

15 LEDs orgánicos (OLEDs)

Carbono con hybridización *sp2*

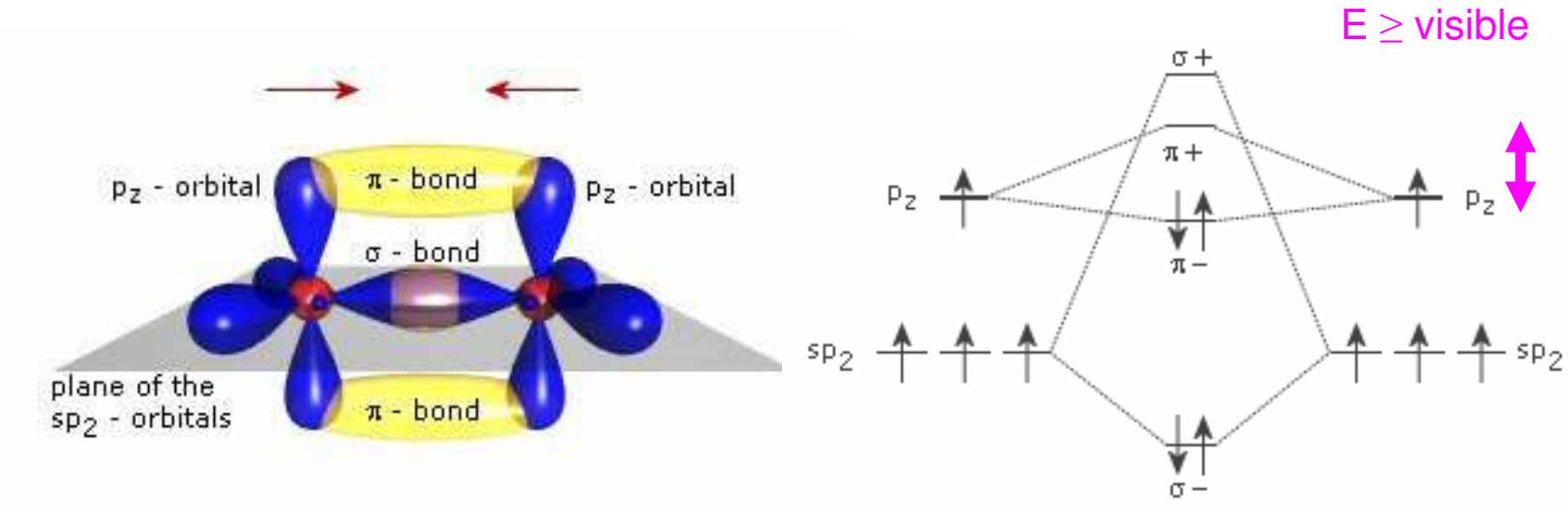

LEDs orgánicos

Pequeñas moléculas orgánicas (tipo benzeno como unidad básica)

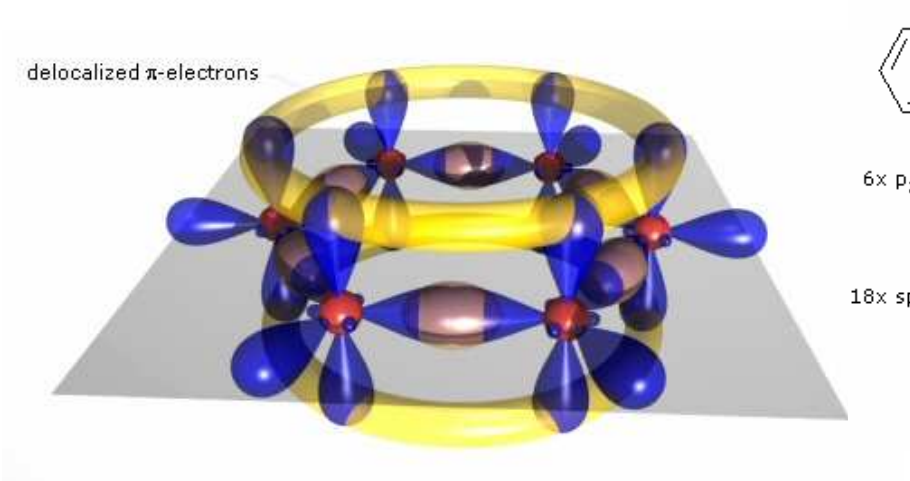

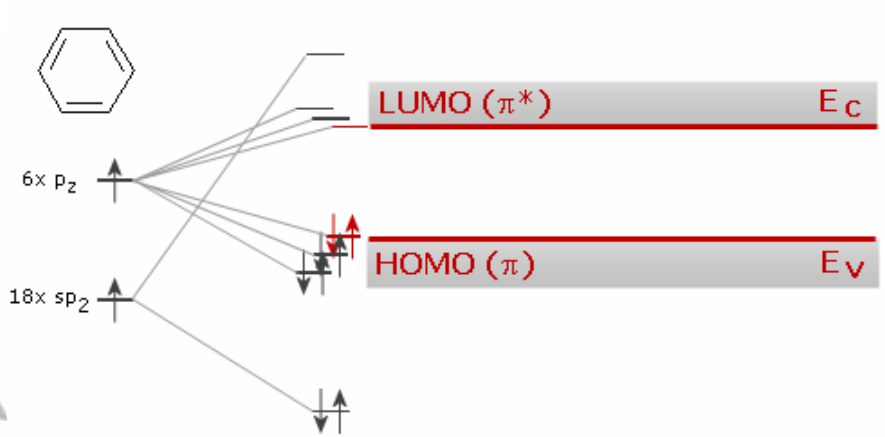

E = visible

lowest unoccupied molecular orbital (LUMO)
highest occupied molecular orbital (HOMO)

LEDs orgánicos

Semiconductores de polímeros orgánicos, cadena 1D
conducción por ‘hopping’ de una cadena a otra

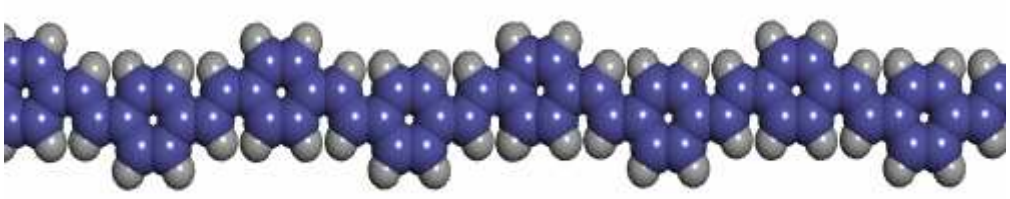

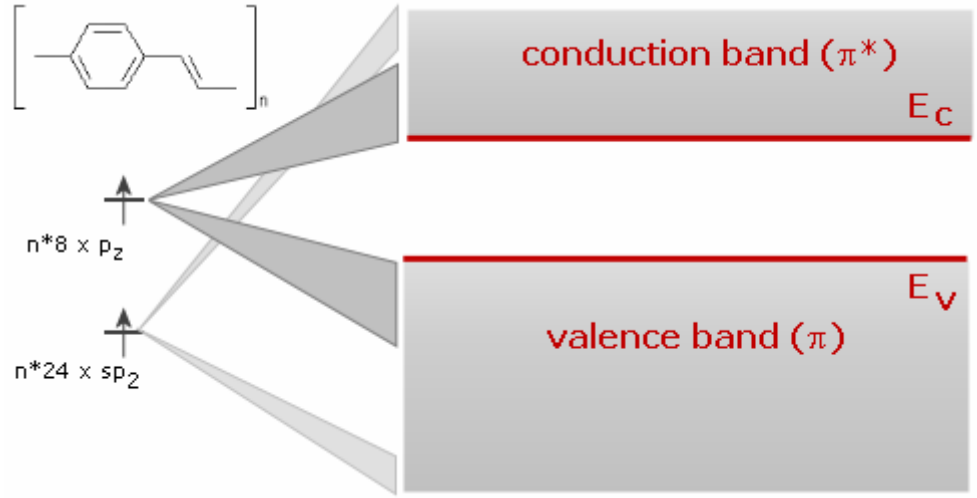

LEDs orgánicos

Funcionamiento de un OLED:

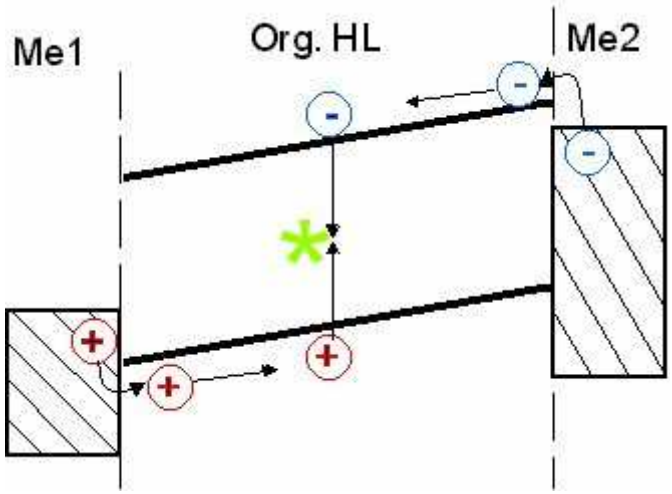

configuración simple:
contactos de diferentes metales

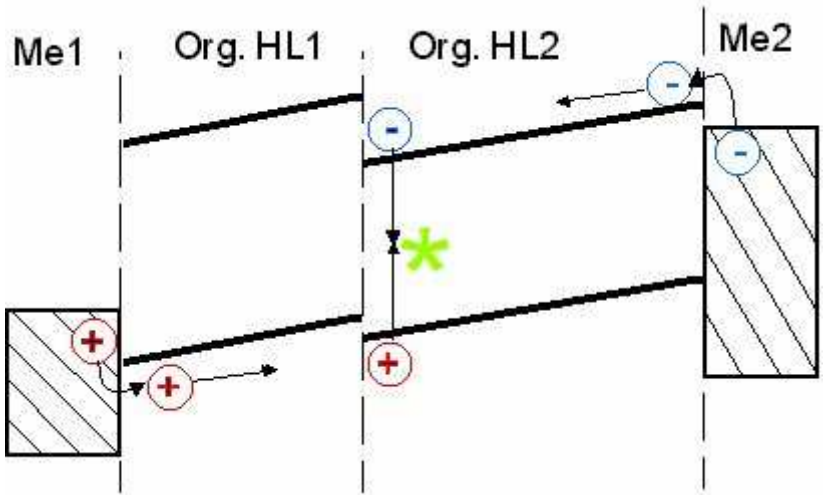

configuración para hacer coincidir electrones y huecos

LEDs orgánicos

Desventaja: vida útil limitada

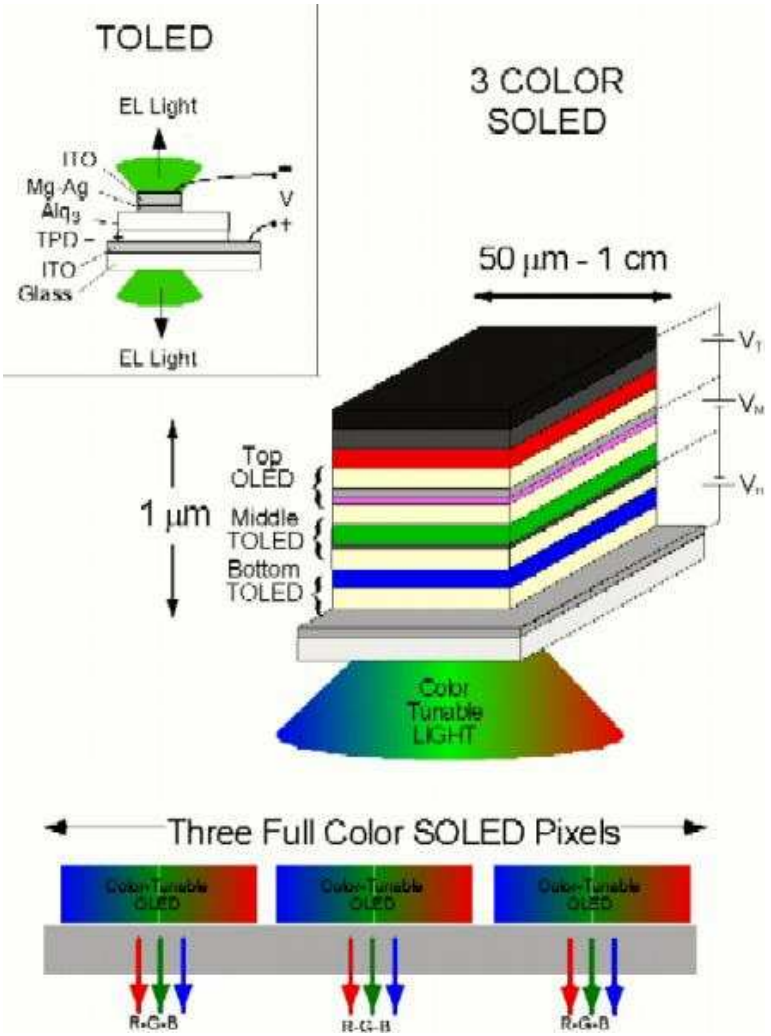

LEDs orgánicos

Pantallas:

Sony

Kodak